



Article

Need for a Standardized Translational Drug Development Platform: Lessons Learned from the Repurposing of Drugs for COVID-19

Frauke Assmus ^{1,2,†}, Jean-Sélim Driouich ^{3,†}, Rana Abdelnabi ^{4,†}, Laura Vangeel ^{4,†}, Franck Touret ^{3,†}, Ayorinde Adehin ^{1,2}, Palang Chotsiri ¹, Maxime Cochin ³, Caroline S. Foo ⁴, Dirk Jochmans ⁴, Seungtaek Kim ⁵, Léa Luciani ³, Grégory Moureau ³, Soonju Park ⁵, Paul-Rémi Petit ³, David Shum ⁵, Thanaporn Wattanakul ¹, Birgit Weynand ⁶, Laurent Fraisse ⁷, Jean-Robert Ioset ⁷, Charles E. Mowbray ⁷, Andrew Owen ⁸, Richard M. Hoggland ^{1,2}, Joel Tarning ^{1,2}, Xavier de Lamballerie ³, Antoine Nougairède ³, Johan Neyts ^{4,9}, Peter Sjö ⁷, Fanny Escudie ^{7,*}, Ivan Scandale ^{7,*} and Eric Chatelain ^{7,*}

- ¹ Mahidol Oxford Tropical Medicine Research Unit, Faculty of Tropical Medicine, Mahidol University, Bangkok 10400, Thailand
- ² Centre for Tropical Medicine and Global Health, Nuffield Department of Medicine, University of Oxford, Oxford OX3 7LG, UK
- ³ Unité des Virus Émergents (UVE), Institut de Recherche pour le Développement (IRD), Aix-Marseille University, 190-Inserm 1207, 13005 Marseille, France
- ⁴ Laboratory of Virology and Chemotherapy, Department of Microbiology, Immunology and Transplantation, Rega Institute for Medical Research, Katholieke Universiteit Leuven, 3000 Leuven, Belgium
- ⁵ Institut Pasteur Korea, 16, Daewangpangyo-ro 712 beon-gil, Bundang-gu, Seongnam-si 13488, Korea
- ⁶ Department of Imaging and Pathology, Katholieke Universiteit Leuven, Translational Cell and Tissue Research, 3000 Leuven, Belgium
- ⁷ Drugs for Neglected Diseases Initiative (DNDi), 1202 Geneva, Switzerland
- ⁸ Centre for Excellence in Long-Acting Therapeutics (CELT), Department of Pharmacology and Therapeutics, University of Liverpool, Liverpool L69 7ZX, UK
- ⁹ Global Virus Network (GVN), Baltimore, MD 21201, USA
- * Correspondence: fescudie@dndi.org (F.E.); iscandale@dndi.org (I.S.); echatelain@dndi.org (E.C.)
- † These authors contributed equally to this work.



Citation: Assmus, F.; Driouich, J.-S.; Abdelnabi, R.; Vangeel, L.; Touret, F.; Adehin, A.; Chotsiri, P.; Cochin, M.; Foo, C.S.; Jochmans, D.; et al. Need for a Standardized Translational Drug Development Platform: Lessons Learned from the Repurposing of Drugs for COVID-19. *Microorganisms* **2022**, *10*, 1639. <https://doi.org/10.3390/microorganisms10081639>

Academic Editor:
Sofia Costa-de-Oliveira

Received: 7 July 2022

Accepted: 4 August 2022

Published: 12 August 2022

Publisher's Note: MDPI stays neutral with regard to jurisdictional claims in published maps and institutional affiliations.



Copyright: © 2022 by the authors. Licensee MDPI, Basel, Switzerland. This article is an open access article distributed under the terms and conditions of the Creative Commons Attribution (CC BY) license (<https://creativecommons.org/licenses/by/4.0/>).

Abstract: In the absence of drugs to treat or prevent COVID-19, drug repurposing can be a valuable strategy. Despite a substantial number of clinical trials, drug repurposing did not deliver on its promise. While success was observed with some repurposed drugs (e.g., remdesivir, dexamethasone, tocilizumab, baricitinib), others failed to show clinical efficacy. One reason is the lack of clear translational processes based on adequate preclinical profiling before clinical evaluation. Combined with limitations of existing in vitro and in vivo models, there is a need for a systematic approach to urgent antiviral drug development in the context of a global pandemic. We implemented a methodology to test repurposed and experimental drugs to generate robust preclinical evidence for further clinical development. This translational drug development platform comprises in vitro, ex vivo, and in vivo models of SARS-CoV-2, along with pharmacokinetic modeling and simulation approaches to evaluate exposure levels in plasma and target organs. Here, we provide examples of identified repurposed antiviral drugs tested within our multidisciplinary collaboration to highlight lessons learned in urgent antiviral drug development during the COVID-19 pandemic. Our data confirm the importance of assessing in vitro and in vivo potency in multiple assays to boost the translatability of pre-clinical data. The value of pharmacokinetic modeling and simulations for compound prioritization is also discussed. We advocate the need for a standardized translational drug development platform for mild-to-moderate COVID-19 to generate preclinical evidence in support of clinical trials. We propose clear prerequisites for progression of drug candidates for repurposing into clinical trials. Further research is needed to gain a deeper understanding of the scope and limitations of the presented translational drug development platform.

Keywords: COVID-19; drug repurposing; translational medicine; pandemics; clinical trials

1. Introduction

The coronavirus Severe Acute Respiratory Syndrome Coronavirus 2 (SARS-CoV-2) is the causative pathogen of COVID-19, one of several coronaviruses that can infect humans, along with SARS-CoV and MERS-CoV [1]. Due to its high infectivity and ability to cause severe disease and death, COVID-19 became a public emergency of international concern and was classified as a pandemic by the World Health Organization (WHO) in March 2020 [2]. At the time of writing, over 537 million confirmed cases and more than 6 million deaths have been recorded globally [3,4], contributing to 14.9 million excess deaths associated with the COVID-19 pandemic [5].

COVID-19 has a polymorphic clinical presentation, ranging from non-specific viral symptoms with fever, cough, dyspnea, vomiting, and fatigue, to isolated upper airway involvement and finally to acute respiratory distress syndrome [6]. Early infection may be initially asymptomatic or evolve in progressive stages (mild and severe). A worsening of symptoms usually occurs 7 to 10 days after initial clinical symptoms, possibly linked to a cytokine storm resulting from a strong immune response and accompanied by a high risk of thrombosis [7].

COVID-19 is a serious respiratory disease. Approximately 80% of patients infected remain mildly symptomatic whilst 20% present more severe symptoms [8]. Patients with severe symptoms may require hospitalization, often with oxygen supplementation in critical cases, invasive ventilation, and Intensive Care Unit (ICU) admission. Worldwide, the SARS-CoV-2 pandemic has placed ICUs under immense strain and led to high mortality, until the availability of vaccines to physicians and at-risk patients by the end of 2020 and to the wider population by the first quarter of 2021. In low resource setting areas, where there is a lack of access to such medical tools and infrastructure, the need to prevent progression to severe COVID-19 is critical. Moreover, disruption in available healthcare systems has exacerbated cases of other diseases, such as malaria, human immunodeficiency virus (HIV), and tuberculosis, reinforcing the importance of quickly treating COVID-19 to decrease the spread of the disease.

DNDi and several expert groups from the COVID-19 Clinical Research Coalition have harmonized efforts to launch the ANTICOV clinical trial platform in multiple African countries [9]. Initiated in May 2020, ANTICOV focused on identifying and proposing repurposing drug candidates to generate data supporting treatment strategies for mild to moderate SARS-CoV-2 patients in low- and middle-income countries [10]. The ANTICOV clinical trial responded to the urgent need to identify treatments for mild and moderate cases of COVID-19 that can be used early to prevent hospitalization spikes that could overwhelm fragile and overburdened health systems. The ultimate goal was to reduce the number of patients progressing to severe COVID-19 requiring hospitalization, thereby relieving the burden on healthcare systems and facilitating the so-called “flattening of the curve”, considering global public health information available at the time through various open-data-sharing platforms, in particular the coronavirus resource center of the Johns Hopkins University of Medicine [4]. This objective applies to existing and subsequent waves of the pandemic in contexts where systematic measures such as quarantine or use of personal protective equipment is not feasible. ANTICOV is a flexible and innovative trial designed for treatments to be added or removed as evidence emerges. The trial accommodates testing for multiple antiviral and anti-inflammatory agents and aims to select the most promising treatments from ongoing global scientific efforts with proof of efficacy.

In the traditional (de novo) drug discovery process, it typically takes 10–17 years to bring a drug to the market, and costs reach approximately USD 800 million [11]. In contrast, drug repurposing (also known as repositioning), facilitates the identification of new medications by investigating currently approved drugs for new therapeutic clinical use [11]. This approach is of particular interest in response to the COVID-19 pandemic emergency, where rapid drug discovery for the management of COVID-19 and prevention of disease progression is crucial. Advantages over the traditional drug discovery and development pipeline include lower associated risks owing to previously established

pre-clinical, pharmacokinetic (PK), and safety profiles. In addition, since clinical data are available at the beginning of a development project, the risks associated with further development are greatly reduced [12]. Hence, repurposed drugs can be fast-tracked through to Phase 3 human clinical trials [13,14], shortening development time frames and lowering investment costs.

Historic examples of successfully repurposed drugs include sildenafil (originally indicated for angina, now indicated for erectile dysfunction) or thalidomide (originally indicated for morning sickness, now indicated for multiple myeloma) [15]. Regarding the treatment of COVID-19, the exploration of drugs from the antiviral field provides logical short-term opportunities to rapidly combat an evolving global pandemic. Repurposing existing drugs to treat COVID-19 is biologically reasonable, as SARS-CoV-2 shares some similarities with other coronaviruses, such as SARS-CoV and MERS-CoV [16]. There are successful precedents in repurposing antivirals for new virus targets [17], and indeed, most of the drugs currently in clinical trials for COVID-19 are repurposed approved antiviral drugs. “Obvious” disease-modifying drugs (i.e., anti-inflammatory drugs) such as dexamethasone or baricitinib were successfully repurposed quickly for severe COVID-19 [18–20]. Anticoagulant and/or antiplatelet therapies have also been assessed during the pandemic, given that venous thromboembolism and thrombosis complications were observed in COVID-19 patients. While survival increase was shown in non-critically ill hospitalized COVID-19 patients receiving anticoagulant therapy, antithrombotic preventive treatment is not recommended for non-hospitalized patients without evidence of venous thromboembolism [21–23]. “Direct repurposing” of existing drugs at the already approved dose was a logical strategy to rapidly identify suitable treatment(s) for the management of severe cases of COVID-19 and to prevent disease progression. Repurposing can also refer to a non-approved dose of an existing drug—“indirect repurposing”—since the approved dose is optimized and selected for another pathogen or indication [24].

Historically, the relevance of drug combination regimens has been demonstrated in the fields of HIV chronic viral infection and cancer [25,26]. Exploring drug combinations for COVID-19 also holds much promise, considering the complexity of the disease pathology. Indeed, using drugs with different mechanisms of action (MoA) to target different aspects of the disease (e.g., reducing viral load with an antiviral and suppressing the cytokine storm with an anti-inflammatory compound or immunomodulator) or different steps in the viral cycle would be expected to improve therapeutic efficacy and allow a much wider patient population with different needs to benefit from treatment [27]. Repurposed antiviral and immunomodulator combination regimens have the potential to serve an urgent need in outpatients, both as prophylaxis and as treatment, and is the current focus of the ANTICOV adaptive platform trial in low resource settings [10].

Leveraging existing assets and networks to fast-forward the development of novel COVID-19 treatments, DNDi designed and implemented a translational drug development platform to generate preclinical evidence in support of treatment arms for the ANTICOV clinical trial. This partnership included well-established virology laboratories and PK modeling expert institutions to systematically evaluate the clinical potential of repurposed drugs. The aim of this COVID-19 translational platform is to catalyze translational and drug repurposing research and accelerate the sharing of data. This includes preclinical data related to *in vitro* and *ex vivo* antiviral potency, *in vivo* efficacy in a hamster infection model, as well as drug metabolism and pharmacokinetic (DMPK) studies of selected repurposed drugs. In addition, the use of pharmacometric modeling and simulation was incorporated for the evaluation of drug exposures in plasma and target organs based on both preclinical and clinical data.

The current article discusses the processes and methodology we implemented in repurposing drugs in the context of the COVID-19 pandemic and provides examples of identified repurposed antiviral drugs that were tested in our multidisciplinary collaboration with the aim of highlighting areas that need finessing in urgent antiviral drug development.

2. Experimental Verification of Repurposed Drugs against COVID-19

As for any drug repurposing development, COVID-19 drug repurposing needed to go through three key stages before progressing to later stages of clinical development: (i) identification of drug candidates, (ii) experimental verification of drug candidates in pre-clinical models, and (iii) assessment of the drug effectiveness in Phase 2 clinical trials [28]. The methodology used in this collaboration to test repurposed and experimental drugs, alone or in combinations, is outlined below (refer to Supplementary Materials—Section S1). The ideal strategy for the generation of new preclinical data for repurposed drugs against SARS-CoV-2 to build a rationale for clinical evaluation is outlined in Figure 1.

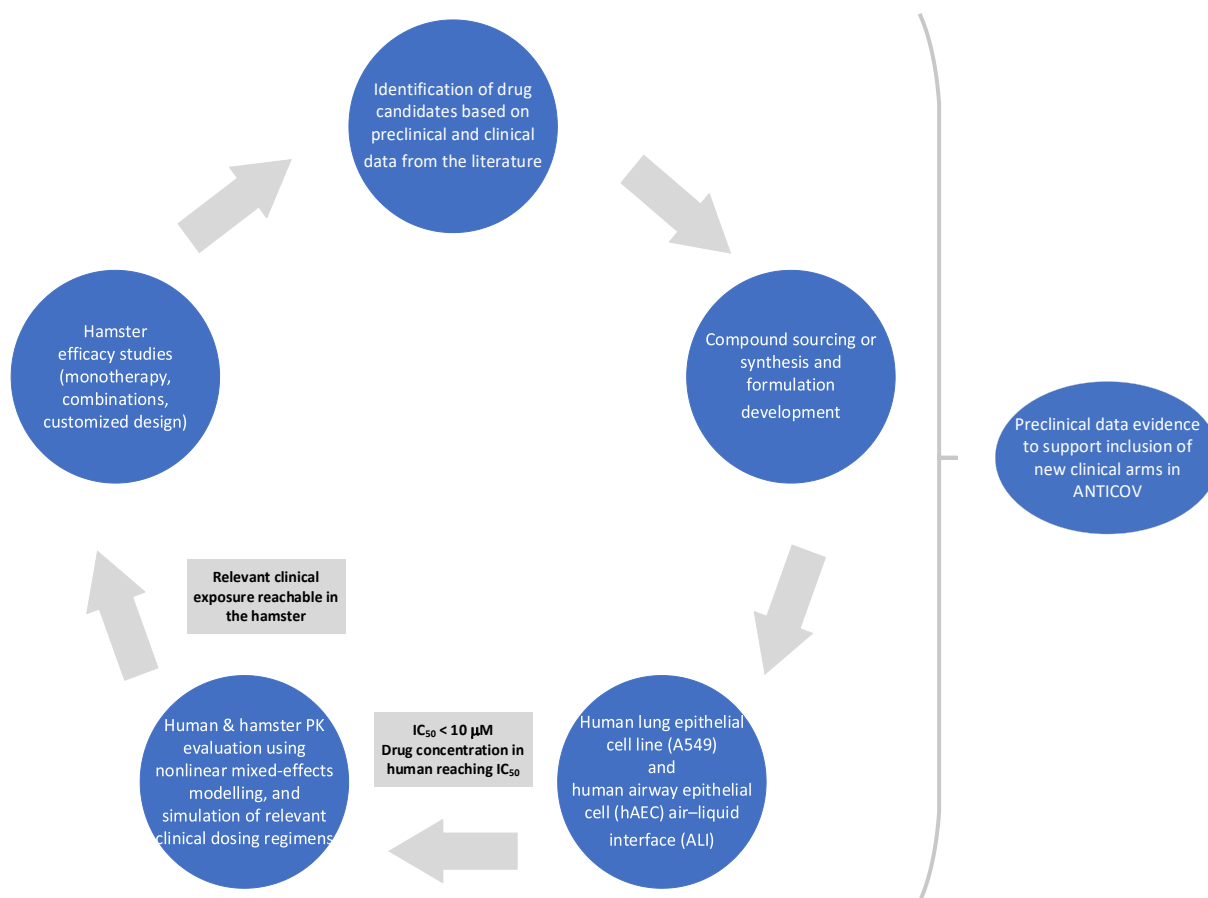


Figure 1. Ideal process for generating new preclinical data of repurposed drugs against SARS-CoV-2 to build a rationale for a clinical evaluation.

2.1. Identification and Selection of Drug Repurposing Candidates for Preclinical Studies

The approach taken by DNDi to identify and select repurposing candidates for entry into the ANTICOV trial platform was based on publicly available literature (for details see Supplementary Materials, Section S1.1). Specific criteria included: (i) potential in vitro activity against SARS-CoV-2; (ii) in vivo efficacy in preclinical species, when available (e.g., antiviral activity of compounds in the Syrian hamster or other appropriate animal models); (iii) their safety in another indication (effects of common comedications or comorbidities as well as risks associated with pregnancy or lactation, and compatibility with anti-inflammatory combination medicines were considered); (iv) route of administration; (v) their ability to be manufactured at scale and at an affordable cost; and (vi) in the best case scenario, preliminary evidence of their activity in mild to moderate SARS-CoV-2 patients from proof-of-concept (PoC) studies, antiviral studies, and modeling data supporting the best dose regimen.

A preliminary longlist of candidates included drugs demonstrated to have *in vitro* antiviral activity against SARS-CoV-2 virus and for which the plasma concentration following approved dosing in humans exceeded that needed for antiviral activity *in vitro*. For antiviral drug candidates, free plasma exposures at the highest dose approved by regulatory agencies (mainly the US Food and Drug Administration [FDA] and the European Medicines Agency [EMA]) were used to estimate the potential to achieve free human plasma coverage above the SARS-CoV-2 antiviral EC₅₀. This provided an initial prioritization of the longlist by excluding/down-selecting compounds with a low probability of achieving clinical antiviral efficacy. Drug protein binding was assumed to be minimal in the *in vitro* system and no correction of the *in vitro* EC₅₀ efficacy was made at this stage; the free drug hypothesis did not always apply, and data should be interpreted with caution and in a drug-specific manner [29]. For the final stage selection, sustained exposure over the *in vitro* antiviral EC₉₀ was targeted. The lung was a key target organ of the SARS-CoV-2 virus during the early stages of the pandemic; therefore, the initial prioritization based on free plasma levels was followed by modeling of local exposure in the lung as described in previous reports [30,31]. Of note, compounds suitable for treatment of late stage COVID-19 were not included in this analysis (e.g., dexamethasone and baricitinib).

During the progress of this work, additional compounds were continuously evaluated and considered for inclusion as new data were made available from preclinical and clinical investigations. This was a highly dynamic period of research during 2020–2021, which witnessed an explosion of activity and rapid sharing of results, often through preprints and other non-peer reviewed releases with higher levels of uncertainty and a greater need for independent corroboration.

The selection of drug repurposing combinations was based on the hypothesis that a combination of a SARS-CoV-2 antiviral compound and an anti-inflammatory agent able to deescalate the inflammatory response caused by the viral infection would maximize the treatment impact and prevent disease progression.

2.2. Generation of Preclinical Data

Following the selection of candidates described above, the following drugs were sourced from various providers: atazanavir, favipiravir, sofosbuvir, ritonavir, nitazoxanide, ambroxol HCl, camostat mesylate, cepharantine, and fluvoxamine maleate from Ambeed Inc., USA; ritonavir, nitazoxanide, atazanavir, N-desethyl-amodiaquine, and nelfinavir from BLD Pharmatech Ltd.; daclatasvir, sofosbuvir and its metabolite, nitazoxanide metabolite tizoxanide, pentoxifylline, and clofazimine from AK Scientific, Union City, CA, USA; nelfinavir mesylate, molnupiravir and its main metabolite from MedChemExpress, Monmouth Junction, NJ, USA; colchicine, amodiaquine, mefloquine HCl, and ivermectin from Carbosynth Ltd., Compton, UK; bemnifosbuvir (free base AT-511, salt AT-527, and its metabolite AT-273) from DC Chemicals, Shanghai, China. Nirmatrelvir was synthesized at TCG Lifesciences Private Ltd., Kolkata, India. Preclinical data were then generated, including pharmacodynamic (PD) *in vitro* assays, *ex vivo* 3D models, and *in vivo* hamster disease models, to test potency against SARS-CoV-2 [32]. Pharmacokinetic data were also generated, including drug exposure in plasma and tissue of interest (lungs). Finally, population PK modeling and simulation was carried out, as described below.

2.2.1. In Vitro/Ex Vivo Activity

In vitro profiling of the selected repurposed and experimental drugs was performed in three different phenotypic virus-cell-based antiviral assays with SARS-CoV-2 in Vero cells (+/– CP-100356, a Pgp-pump inhibitor), Calu-3 cells using SARS-CoV-2/KCDC03 (Wuhan strain), and A549-Dual™ hACE2-TMPRSS2 cells using SARS-CoV-2-B.1.1.7 (Alpha variant). Methods and protocols were rapidly adapted from previous antiviral screening campaigns (MERS, SARS-CoV) for developing approaches to identify antivirals against SARS-CoV-2. These assays were designed to determine the effect of small molecules on the infection and replication of SARS-CoV-2 and relied either on the assessment of the cytopathic effect (CPE)

of the virus or on quantification of the viral N protein (immunofluorescence-based assay) in the presence of different drug concentrations. Experimental details are provided in the Supplementary Materials (Section S1.2).

Ex vivo 3D modeling was carried out using Human Airway Epithelia (HAE) in human Air Liquid Interface (ALI) cultures (Mucil AIR—Epithelix™) infected with SARS-CoV-2 ancestral strain B.1 (Bavpat1) or B.1.1.7 (Alpha variant). These differentiated ALI models were designed to study respiratory virus pathogenesis and to evaluate antiviral toxicity and efficacy. The model holds in vitro specific mechanisms to counter invaders comparable to the in vivo situation, such as mucus production, mucociliary clearance, and secretion of defensive molecules [33]. Experimental details are provided in the Supplementary Materials (Section S1.3).

2.2.2. In Vivo Efficacy in Hamsters

In vivo efficacy studies for all tested drugs were conducted in hamsters. Features associated with SARS-CoV-2 infection in hamsters recapitulate some characteristics found in humans with mild SARS-CoV-2 infections; the hamster model was therefore considered an adequate animal model for these studies (hamster pathology description following infection and experimental details are provided in Supplementary Materials and references therein, Section S1.4, Table S1). Modeling of the relevant clinical dosing regimen was selected based on the labels of the considered drugs, assuming 10 days of dosing in line with the target product profile [34]. The hamster infection model of SARS-CoV-2 was used as previously described [35–37] using either the Wuhan strain, the ancestral SARS-CoV-2 B.1 (Bavpat1), or SARS-CoV-2-B.1.351 (Beta variant) strains. Drugs were administered to infected hamsters as homogenous suspensions in their adequate respective vehicle. Groups of 6 hamsters were infected intranasally with 10^4 TCID₅₀ of SARS-CoV-2. Groups of 6 animals received oral doses of repurposed drugs based on body weight. The negative control groups of 6 hamsters were treated with the respective vehicle. Lastly, the positive control groups of 6 animals were treated with favipiravir intraperitoneally (926 mg/kg/day BID), based on doses identified in a hamster model by Driouich et al. [38]. Following infection, hamsters were treated for 3 days, on day 0, day 1, and day 2 post-infection (dpi). Infectious titers were measured using a TCID₅₀ assay, and the viral RNA yields were measured by quantitative real-time PCR in clarified lung homogenates or plasma.

The impact of repurposed drugs on lung pathological changes induced by SARS-CoV-2 was also independently explored. Groups of 4 hamsters were treated orally with the selected repurposed drug. Untreated groups of 4 hamsters received the corresponding vehicle BID. Animals were sacrificed at 5 dpi and based on severity of lung inflammation, alveolar hemorrhagic necrosis, and vessel lesions, a cumulative score from 0 to 10 was calculated and assigned to a severity grading (0 = normal; 1 = mild; 2 = moderate; 3 = marked; 4 = severe; refer to experimental details provided in Supplementary Materials, Section S1.4.1).

2.2.3. Protein Binding and Correction of IC₅₀ Values for Protein Binding

Plasma protein binding of repurposed drugs in hamsters and humans was either measured by the Rapid Equilibrium Dialysis (RED) as described in Abdelnabi et al. [35] or was available from the literature. In addition, binding to assay medium (2% serum DMEM supplemented with 2% *v/v* FCS) in antiviral assays (A549-ACE2TMPRSS2 cells) was determined by RED. In vitro IC₅₀ values were first corrected for protein binding in assay media according to:

$$IC_{50\text{unbound}} = IC_{50\text{media}} \times f_{\text{unbound, media}}, \quad (1)$$

where $IC_{50\text{unbound}}$ is the free drug concentration needed to achieve 50% inhibition of the virus-reduced enhanced green fluorescent protein (eGFP) signals compared with the untreated virus-infected control cells, and $f_{\text{unbound, media}}$ is the unbound drug fraction in assay media.

In a second step, values were scaled to represent the total plasma concentrations in humans or hamsters needed to achieve 50% of the maximum effect, according to:

$$IC_{50 \text{ plasma}} = IC_{50 \text{ unbound}} / f_{\text{unbound, plasma}}, \quad (2)$$

where $f_{\text{unbound, plasma}}$ is the unbound drug fraction in plasma.

2.2.4. Pharmacokinetic Studies in Hamster

Pharmacokinetics of selected drugs were assessed in uninfected female LGV Golden Syrian hamsters (satellite PK study) purchased from Beijing Vital River Laboratory Animal Technology Co., Ltd. (Beijing, China) or Envigo (Indianapolis, Indiana, USA). Details regarding dosing regimen, drug formulation, PK sampling time points, as well as bioanalytical procedures are provided in the Supplementary Materials (Experimental details Section S1.5, Tables S2 and S3). Briefly, most drugs were given as a single dose by oral gavage except for nelfinavir (intraperitoneally), amodiaquine, and ivermectin (both oral and subcutaneous administration). For nelfinavir and atazanavir (ritonavir-boosted), single and multiple dose PK studies were performed. Three dose levels (triplicate experiments in each dose level) were tested for the majority of drugs, with doses ranging from 1 to 200 mg/kg, depending on the drug. For nelfinavir and ivermectin, PK profiles at two dose levels were assessed. Blood samples (1–7 samples per hamster, depending on the drug) were collected and drug concentrations analyzed with a LC–MS/MS method, which was optimized for the various drugs.

2.2.5. Population Pharmacokinetic Analysis

For each drug, plasma concentration–time profiles from satellite PK studies in hamsters were pooled and analyzed using a nonlinear mixed-effects modeling approach in NONMEM, v7.4 (Icon Development Solution, Ellicott City, MD, USA). Details regarding model development and validation are provided in the Supplementary Materials—Experimental details, Section S1.6.1. Briefly, different absorption, disposition, and variability models were evaluated. To improve the translational aspect of the model, body weight was implemented a priori as an allometric function. Moreover, dose and (if applicable) different routes of administration were evaluated as covariates. Parent and metabolite data (if available) were analyzed simultaneously, assuming complete *in vivo* conversion.

In addition to the population PK analysis in hamsters, a literature search was performed to identify available PK information in humans [39]. Details regarding the model selection (if a population PK model was published) or model derivation (based on non-compartmental PK analysis or digitized PK data) are provided in the Supplementary Materials, Section S1.6.2.

2.2.6. Population Pharmacokinetic Simulations

PK parameters from the final population PK models in humans and hamsters were used to simulate plasma exposures for various dosing scenarios. Simulations were performed with the *mlxR* package in the R software [40], for a treatment duration of 10 days in both hamsters and humans. A total of 1000 hypothetical individuals (body weight of 70 kg) or hamsters (body weight 120 g) were simulated for each dosing scenario.

For the simulations in humans, inter-individual variability (IIV) as reported in clinical PK models was implemented (when available). Otherwise, an IIV of 15% was assumed for all PK parameters (in humans and hamsters) to reflect an expected population variability. Simulations of plasma exposure in humans were based on the standard (clinical) dose given once or twice daily according to the general practice. A loading dose was not considered.

Dosing scenarios for simulations in hamsters correspond to the dose range tested in the satellite PK studies in hamster; and twice daily dosing was assumed (Supplementary Materials Figures S1–S17 for pharmacokinetic profiles in hamsters). When required, extrapolation beyond this dose range was performed to identify doses in hamsters

that reach drug exposure in humans at clinically relevant doses. Peak concentrations (C_{\max}) and cumulative areas under the concentration-time curves (AUC_{total}) were extracted and used for comparison with clinical simulations. Boxplots of simulated C_{\max} in humans and hamsters were overlaid with the *in vitro* IC_{50} values reported in A549-ACE2TMPRSS2 cells. These IC_{50} values were corrected for protein binding (see above) to compare simulated C_{\max} from the developed PK models with expected therapeutic concentrations.

3. Results

3.1. Selected Repurposed Drugs for Further Evaluation

The initial longlist of antiviral drug candidates identified 88 compounds for further investigation. Following the prioritization process using criteria listed in 2.1 (Identification and selection of drug repurposing candidates for preclinical studies), 25 compounds were selected as potential candidates for inclusion in the ANTICOV study (Supplementary Materials, Results Section S2.1, Table S4). Remdesivir was not considered further because its administration mode by infusion in humans was not considered adequate for inclusion in ANTICOV; moreover, it was not deemed a suitable control for Syrian hamster experiments due to difficulty of administration and lack of efficacy in standard rodent animal models of SARS-CoV-2 infection related to poor plasma stability in this species. The remaining compounds were further evaluated in the preclinical investigations summarized in Table 1. Selected repurposed drugs were grouped according to compound class for single agents (Table 1), namely direct-acting antivirals (DAAs) and indirect-acting antivirals (IAA). The selected drug candidates covered a wide variety of MoAs. DAA compounds included HIV protease inhibitors, RNA viral polymerase inhibitors, hepatitis C virus (HCV) NS5A inhibitors, protease (Mpro) inhibitors, and nucleotide polymerase inhibitors. IAA compounds comprised mucolytic, antimalarial, ACE binding, anti-inflammatory, anti-parasitic, and vasodilatory drugs as well as selective serotonin reuptake (SSRI) inhibitors or combinations thereof (Table 2).

Based on the outcome of an expert panel discussion involving representatives from various organisations (Access to COVID-19 Tools Accelerator [ACT-A] Therapeutics Partnership, Unitaid, Wellcome on behalf of the ACT-A), the following drug combinations were initially prioritized: atazanavir/ritonavir (ATZ/r) + nitazoxanide; favipiravir + ATZ/r; favipiravir + nitazoxanide; and sofosbuvir/daclatasvir. During the project, we continuously reviewed new options and promising additional re-purposed drug candidates or drug combinations based on newly generated preclinical and proof-of-concept clinical data. Clinical results highlighted a potential for inhaled steroids, budesonide and ciclesonide, in COVID-19; these were selected as the primary anti-inflammatory combination partners for the ANTICOV trials [41–43]. However, inhaled steroids were not assessed in our translational platform, as drug delivery by inhalation was not deemed suitable for assessment in animal models. Ongoing review highlighted the rationale and potential for the following combinations, which were further assessed preclinically: amodiaquine + ivermectin following data showing potential for a combination [44]; nelfinavir + cepharantine, selected following published *in vitro* data highlighting a potential synergistic effect of this combination in limiting SARS-CoV-2 proliferation [45] and the impact of nelfinavir on lung inflammation in animal models, although it had no impact on SARS-CoV-2 viral load [46]; and clofazimine, selected for combination with the experimental drug molnupiravir, because it showed anti-SARS-CoV-2 potency *in vitro* in Vero cells and the property to accumulate in the lung [47,48].

Table 1. Overview of prioritized repurposed drugs and generated preclinical data—Single agents.

Repurposed Drug/Experimental Compound	Mechanism of Action; Target	Activity In Vitro; Potency EC ₅₀ or IC ₅₀ < 10 μM			Activity Ex Vivo Human Airway Epithelia (HAE)	Exposure in Human at Clinically Relevant Dose and Matching Doses in Hamster ^a			Activity and Exposure in Hamster Infection Model of SARS-CoV-2			
		Vero Cells	Calu-3 Cells	A549 Cells		C _{max} Human above IC ₅₀ at Clinically Relevant Dose	C _{max} Hamster above IC ₅₀ for Dose Matching C _{max} in Human	C _{max} Hamster above IC ₅₀ for Dose Matching AUC in Human	Activity in SARS-CoV-2 Hamster Model	Dose(s) per Occasion, Frequency, Duration	C _{max} Hamster above IC ₅₀ ^b	C _{min} Hamster above IC ₅₀ for >24 h ^b
Direct Acting Antivirals (DAA)												
Atazanavir (ritonavir-boosted)	HIV protease inhibitors	No	No	No	No	No	No (24 mg/kg)	No (72 mg/kg)	No	48 mg/kg (16 mg/kg ritonavir), BID, 3–4 days	No (48/16 ritonavir mg/kg, BID)	No (48/16 mg/kg ritonavir, BID)
Bemnifosbuvir (AT-527/AT-511) (experimental cpd) ^c	RdRp (guanosine nucleotide analogue)	No	No	No	No	Yes		ND	No ^d	150–250 mg/kg, BID, 3 days	No (250 mg/kg, BID)	No (250 mg/kg, BID)
Daclatasvir	HCV NS5A inhibitor (polymerase inhibitor)	Yes ^{P_{GP}, T}	No	No ^T	No	No	No (10 mg/kg)	No (15 mg/kg)	No	25 mg/kg, BID, 3 days	No (25 mg/kg, BID)	No (25 mg/kg, BID)
Favipiravir	RNA-dependent RNA polymerase (RdRp),	No	No	No	No	No	Yes (25 mg/kg)	Yes (25 mg/kg)	Yes	300 mg/kg, BID, 4 days; 462.5 mg/kg, BID, 3 days	Yes (300 mg/kg, BID)	No (300 mg/kg, BID)
Molnupiravir and metabolite EIDD-1931, experimental cpd/Merck)	RdRp (hydroxy-cytidine nucleotide analogue)	Yes ^{P_{GP}}	Yes	Yes	Yes (10 μM)	Yes	Yes (50 mg/kg)	Yes (150 mg/kg)	Yes	75–200 mg/kg, BID, 3–4 days	Yes (150 mg/kg BID)	No (150 mg/kg BID)
Nelfinavir	HIV protease inhibitors	Yes ^T	Yes (borderline, 13 μM)	Yes ^T	Yes	No	No (70 mg/kg)	No (100 mg/kg)	No ^e	100 mg/kg, QD, cepharanthine boosted (50 mg/kg, BID)	No (100 mg/kg)	No (100 mg/kg)
Nirmatrelvir (experimental cpd/Pfizer) [35]	Mpro inhibitor	Yes	Yes	Yes	Yes (1 μM)			ND	Yes	125–250 mg/kg, BID, 4 days	Yes (125 mg/kg, BID)	Yes (125 mg/kg, BID)
Sofosbuvir	HCV NS5B inhibitor (polymerase inhibitor)	No	No	No	No	No	No (>200 mg/kg)	No (>200 mg/kg)	No	100 mg/kg, QD, 3 days	No (100 mg/kg)	No (100 mg/kg)
Other Mechanisms of Action—Indirect Acting Antivirals												
Ambroxol	Mucolytic/prevent virus to bind to ACE-2 receptor	No	No	No	No	No	No (30 mg/kg)	No (50 mg/kg)	No	50 mg/kg, BID, 3 days	No (50 mg/kg BID)	No (50 mg/kg BID)
Amodiaquine ^f	Anti-malarial	Yes (~10 μM)	No	No	No	No	No (<5 mg/kg)	No (<5 mg/kg)	No (parent)	50–100 mg/kg, QD, 4–5 days	No (100 mg/kg)	No (100 mg/kg)

Table 1. Cont.

Repurposed Drug/Experimental Compound	Mechanism of Action; Target	Activity In Vitro; Potency EC ₅₀ or IC ₅₀ < 10 µM			Activity Ex Vivo Human Airway Epithelia (HAE)	Exposure in Human at Clinically Relevant Dose and Matching Doses in Hamster ^a			Activity and Exposure in Hamster Infection Model of SARS-CoV-2			
		Vero Cells	Calu-3 Cells	A549 Cells		C _{max} Human above IC ₅₀ at Clinically Relevant Dose	C _{max} Hamster above IC ₅₀ for Dose Matching C _{max} in Human	C _{max} Hamster above IC ₅₀ for Dose Matching AUC in Human	Activity in SARS-CoV-2 Hamster Model	Dose(s) per Occasion, Frequency, Duration	C _{max} Hamster above IC ₅₀ ^b	C _{min} Hamster above IC ₅₀ for >24 h ^b
Cepharanthine	Block virus entry/ ACE2 binding	Yes ^T	No	No	No	No	No (1 mg/kg)	No (1 mg/kg)	No	100 mg/kg, QD, 4 days	No (100 mg/kg)	No (100 mg/kg)
Camostat mesylate	TMPRSS2 inhibitor	No	Yes	No	Yes (10 µM)		ND		No	200 mg/kg, BID, 4 days		ND
Clofazimine	TB inhibitor/ accumulate in lungs	Yes ^T	Yes	Yes ^T	No	No	No (1 mg/kg)	No (1 mg/kg)	No	25 mg/kg, QD, 4 days	Yes (25 mg/kg)	No (25 mg/kg)
Colchicine	Anti-inflammatory	Yes ^T	Yes ^T	Yes ^T	No		ND				NT	
Fluoxetine	SSRI (selective serotonin reuptake inhibitor)	Yes ^T	No	No	No	No	No (10 mg/kg)	No (10 mg/kg)	No	10–100 mg/kg, QD, 4 days	No (100 mg/kg)	No (100 mg/kg)
Fluvoxamine maleate	SSRI (selective serotonin reuptake inhibitor)	No	No	No	No	No	No (12 mg/kg)	No (20 mg/kg)	No	100 mg/kg, QD, 3 days; 200 mg, BID, 4 days	No [§] (100 mg/kg)	No [§] (100 mg/kg)
Ivermectin (oral)	Anti-parasitic drug, Anti-inflammatory	Yes ^T	Yes	Yes ^T	Yes ^T	No	No (0.1 mg/kg)	No (0.1 mg/kg)			NT	
Ivermectin (s.c.)		No	No	No	No	No	No (0.1 mg/kg)	No (0.1 mg/kg)	No	0.4 mg/kg, QD, 1 day or 4 days	No (0.4 mg/kg)	No (0.4 mg/kg)
Mefloquine	Anti-malarial	Yes ^T	No	No	No		ND				NT	
Nitazoxanide (and metabolite tizoxanide)	Antiprotozoal agent (<i>Giardia</i> , <i>Cryptosporidium</i> infections)	Yes	Yes ^{P&P}	No	Yes	No	No (25 mg/kg)	No (150 mg/kg)	No	250 mg/kg, BID, 3–4 days	No (250 mg/kg BID)	No (250 mg/kg BID)

Table 1. Cont.

Repurposed Drug/Experimental Compound	Mechanism of Action; Target	Activity In Vitro; Potency EC ₅₀ or IC ₅₀ < 10 µM			Activity Ex Vivo Human Airway Epithelia (HAE)	Exposure in Human at Clinically Relevant Dose and Matching Doses in Hamster ^a			Activity and Exposure in Hamster Infection Model of SARS-CoV-2			
		Vero Cells	Calu-3 Cells	A549 Cells		C _{max} Human above IC ₅₀ at Clinically Relevant Dose	C _{max} Hamster above IC ₅₀ for Dose Matching C _{max} in Human	C _{max} Hamster above IC ₅₀ for Dose Matching AUC in Human	Activity in SARS-CoV-2 Hamster Model	Dose(s) per Occasion, Frequency, Duration	C _{max} Hamster above IC ₅₀ ^b	C _{min} Hamster above IC ₅₀ for >24 h ^b
Pentoxifylline	Vasodilator; anti-inflammatory	No	No	No	No		ND				NT	
Probenecid	Anti-gout?	No	No	No	No		ND				NT	
Proxalutamide	Androgen receptor antagonist, Anti-inflammatory	No ^T	No	No ^T	No		ND				NT	

^a Plasma exposure in humans at clinically relevant dose (once or twice daily dosing, according to the product information) and hamsters (twice daily dosing) were simulated using population pharmacokinetic models listed in the Supplementary Materials (Table S28). Simulations were performed for a total treatment duration of 10 days. Dosing information in humans is provided in Table S28, along with details for derivation of doses in hamsters matching C_{max} and AUC_{total} in humans (doses provided in brackets). IC₅₀ refers to in vitro activity in A549-ACE2TMPRSS2 cells (if not otherwise indicated) and following correction for protein binding in medium and human/hamster plasma (Supplementary Materials, Table S7). ^b Dose in hamsters used for simulations of C_{max} refer to the maximum dose tested in the hamster infection model of SARS-CoV-2 (if no activity was observed) or the minimum efficacious dose. Twice daily dosing was assumed for simulations. ^c AT-273 is AT-527 metabolite measured in plasma and used as a surrogate for AT-527 plasma concentration; human PK parameters based on literature data. ^d no activity in hamster, except for significant reduction in RNA Yields plasma log₁₀ [copies/mL]; ^e no effect on virus load, but effect on lung inflammation and “disease” outcome; ^f IC₅₀ data for Des-Ethyl-Amodiaquine (=amodiaquine metabolite) not available; ^g P_{gp} in vitro assay was performed in the presence of a P-glycoprotein inhibitor; ^T toxicity observed; highlighted in blue: exposure (C_{max} or C_{min}) above IC₅₀ in hamsters or humans and/or activity in the hamster infection model of SARS-CoV-2; AUC, area under the plasma concentration-time curve; BID, twice daily; C_{max}, peak plasma concentration; cpd, compound; DHE, Des-Ethyl-Amodiaquine (=amodiaquine metabolite); EC₅₀ and IC₅₀, effective or inhibitory concentration leading to half-maximum activity (when not generated experimentally, IC₅₀ were derived from literature (see also Table S1); HCV, hepatitis C virus; HIV, human immunodeficiency virus; NA, not applicable; ND, not determined; NT, not tested; PD, pharmacodynamic; QD, once daily; r, ritonavir; RdRp, RNA-dependent RNA polymerase; s.c., subcutaneous; TB, tuberculosis; § 200 mg/kg dose was toxic.

Table 2. Overview of prioritized repurposed drugs and generated preclinical data- Combination regimen.

	Mode of Action	Dose (mg/kg/day)	Efficacy In Vivo SARS-CoV-2 Hamster Model	Comments
Atazanavir /ritonavir (ATZ/r) /Nitazoxanide	DAA/IAA combination	96/32/500 mg/kg/day	No	
FAV/ATZ/r	DAAs combination	600/96/32 mg/kg/day	Yes	No additive or synergistic activity as compared with FAV alone
FAV/Nitazoxanide	DAA/IAA combination	600/500 mg/kg/day	Yes	No additive or synergistic activity as compared with FAV alone
Sofosbuvir/daclatasvir	DAAs combination	100/100 mg/kg/day	No	
Nelfinavir/Cepharantine	DAA/IAA combination	100/100 mg/kg/day	No	
Ivermectin/Amodiaquine	DAA (considered)/IAA combination	0.4/50 mg/kg/day	No	
Molnupiravir/Clofazimine	DAA/IAA combination	150/25 mg/kg/day	Yes	No additive or synergistic activity as compared with Molnupiravir alone
Molnupiravir/Nirmatrelvir	DAA/DAA combination	150/250 mg/kg/day	Yes	No additive or synergistic activity as compared with nirmatrelvir alone Additive effect as compared with Molnupiravir alone

ATZ, atazanavir; DAA, direct acting antiviral; FAV, favipiravir; IAA, indirect acting antiviral; r, ritonavir.

3.2. Preclinical Data Generated for DAAs

The in vitro antiviral activity of all selected drugs was assessed using three different cell lines, namely Vero kidney epithelial cells (extracted from an African green monkey), Calu-3 cells (extracted from male hepatoma tissue), and A549 cells (adenocarcinoma human alveolar basal epithelial cells). Results are depicted in Table 1, and more details including standard deviations are provided in Supplementary Materials (Results Section S2.2, Table S5).

Regarding the selected DAA compounds, only molnupiravir (RNA-dependent RNA polymerase (RdRp) inhibitor) and its metabolite EIDD-1931 as well as nirmatrelvir (SARS-CoV-2 main protease—Mpro also known as 3CLpro-inhibitor) showed high potency (in the following defined as EC₅₀ or IC₅₀ < 10 μM) in all three in vitro assays without limitations of toxicity. Notably, molnupiravir potency (IC₅₀ < 10 μM) was only reached in the presence of P-gp efflux inhibition. With respect to nelfinavir, high potency in Vero cells and the A549 cell was associated with some toxicity, complicating the distinction between the antiviral effect versus overall toxicity (Table 1). Similarly, daclatasvir showed high potency associated with toxicity in Vero cells, while no potency was observed in the other cell lines. None of the other DAA compounds (atazanavir, bemnifosbuvir, favipiravir, and sofosbuvir) demonstrated potency in the investigated cell lines (Table 1).

The ranking observed for the DAA compounds based on the in vitro cellular assays was consistent with the screening assessment in primary human airway epithelial cells (HAE): molnupiravir (10 μM), nirmatrelvir (1 μM), and nelfinavir (10 μM) were the only DAA compounds that completely inhibited viral replication for the entire duration of the experiment (4 days) when added to the culture medium at the basolateral site of the ALI 1 h before infection (Supplementary Materials, Results Section S2.3, Table S6).

To verify whether human exposure under standard clinical regimens reached target concentrations, population PK modeling was applied. Exposure targets (C_{max} above IC₅₀ under clinical dosing regimen) were set to in vitro IC₅₀ values reported in A549-ACE2TMPRSS2 cells, which were corrected for protein binding (Supplementary Materials

Section S2.4, Table S7). In addition to modeling and simulation of human exposure, population PK models based on hamster PK studies were developed for comparative evaluation of plasma exposures. Plasma concentration—time profiles in hamsters used for the development of population PK models for each drug are shown in the Supplementary Materials (Section S2.5, Figures S1–S17). Examples of structural models, including model parameterizations, are provided in the Supplementary Materials (Section S2.6, Figures S18 and S19). All structural models and covariate effects for both humans and hamsters are summarized in the Supplementary Materials (Section S2.6, Table S8), along with the respective population PK parameters (Section S2.6, Tables S9–S27). Simulations with the final population PK model were used to specify the dose range in hamsters matching human exposure in plasma (C_{\max} and AUC_{total}) under a standard clinical dosing regimen (Supplementary Materials, Section S2.6, Table S28). An example of simulated plasma concentration—time profiles in both humans and hamsters is shown in Figure 2 (molnupiravir metabolite EIDD-1931); the corresponding boxplots with simulated C_{\max} (overlaid with exposure targets) and AUC_{total} in humans and hamsters are shown in Figure 3. The wider dose range in Figure 3 illustrates the screening process to identify doses in hamsters matching drug exposure in humans at a clinically relevant dose. Boxplots with secondary PK parameters for all other investigated compounds are provided in the Supplementary Materials (Section S2.7, Figures S20–S34).

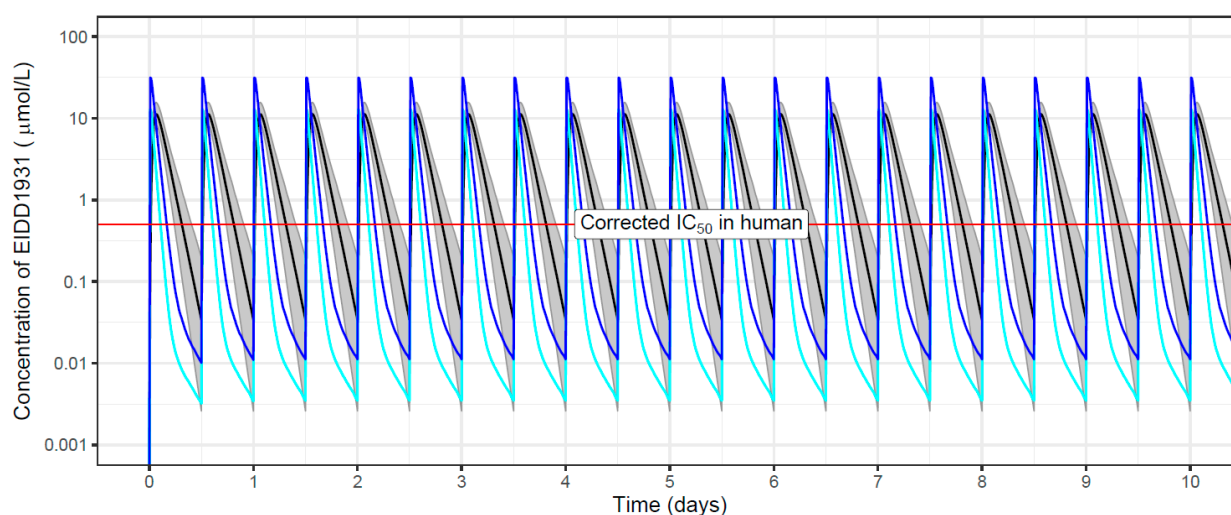


Figure 2. Simulated plasma concentration–time profiles for the molnupiravir metabolite EIDD-1931 in humans (70 kg) and hamsters (120 g), based on the final population pharmacokinetic models (for details, see Supplementary Materials, Section S2.6, Tables S8, S23 and S24). The black line (bounded by a grey shade showing the 90% confidence interval) represents the median simulated concentration-vs.-time profile in humans at a clinically relevant dose (800 mg molnupiravir, twice daily, for 10 days). The cyan line represents the median profile in hamsters, following administration of 50 mg/kg molnupiravir, twice daily for 10 days, corresponding to the approximate dose in hamsters matching C_{\max} in humans. The dark blue line represents the median profile in hamsters following administration of 150 mg/kg molnupiravir, twice daily for 10 days, corresponding to the approximate dose in hamsters matching AUC_{total} in humans; 150 mg/kg twice daily was also the efficacious dose in the hamster infection model of SARS-CoV-2. The horizontal red line denotes the IC_{50} (A549-ACE2TMPRSS2 cells), corrected for plasma protein binding in hamsters and humans (Supplementary Materials, Section S2.4, Table S7).

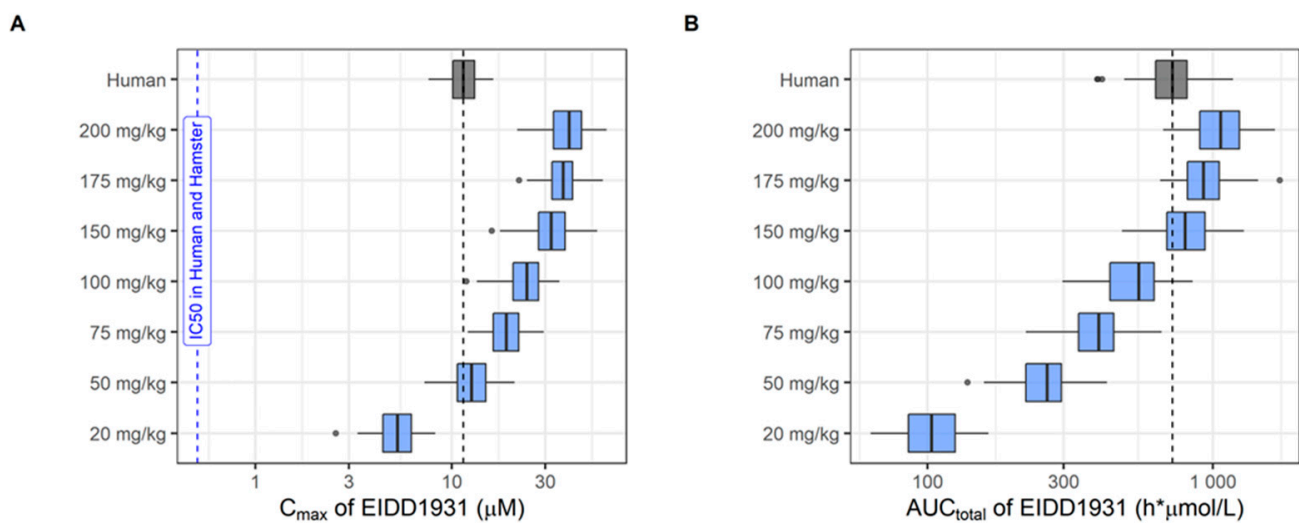


Figure 3. Simulated pharmacokinetic parameters of molnupiravir in humans and hamsters: (A) C_{max} ; (B) AUC_{total} . Predicted pharmacokinetic parameters, i.e., C_{max} and AUC_{total} , in humans receiving 800 mg of molnupiravir twice daily for 10 days (grey box) were compared with pharmacokinetic parameters of hamsters receiving 20 to 200 mg/kg of molnupiravir twice daily (blue boxes) for same number of days. Boxes and whiskers represent the median with inter-quantile range and the 95% prediction intervals, respectively. The blue vertical line denotes the IC_{50} (A549-ACE2TMPRSS2 cells) corrected for plasma protein binding in hamsters and humans.

Regarding drug exposure in humans at a clinically relevant dose, only molnupiravir showed simulated median C_{max} values above the IC_{50} corrected for protein binding. This was not assessed for nirmatrelvir because clinical data were not available at the time. In hamsters, favipiravir also reached exposure targets (at a dose matching human exposure). It is interesting to note that for those compounds for which C_{max} exceed exposure targets in either humans or hamsters, clinical efficacy was also observed.

For in vivo efficacy studies in hamsters, higher doses compared to doses matching human exposure were used, except for nelfinavir and sofosbuvir. For example, a dose-escalation study for molnupiravir with up to 200 mg/kg BID for 4 days was performed to test efficacy. However, only a few DAA compounds demonstrated in vivo efficacy in hamsters despite testing higher doses, including favipiravir, molnupiravir, and nirmatrelvir (Supplementary Materials Figures S35–S46). These compounds also reached target exposures (C_{max} above the IC_{50}) in hamsters at efficacious dosing regimens (Table 1). Conversely, compounds failing to reach target exposures in hamsters in the PD experiments also showed no activity in the hamster efficacy model (daclatasvir, atazanavir, and sofosbuvir). Extended exposure with trough concentrations (C_{min}) above IC_{50} for more than 24 h was only observed with nirmatrelvir. For nelfinavir, no effect on viral load was detected, but a diminution of lung inflammation and “disease outcome” was nevertheless observed.

Although systematic PK/PD analyses were not performed at this stage, some trends regarding the PD driver linking preclinical and clinical activity could be observed, whereby the following parameters were evaluated: exposure in hamsters above IC_{50} for 24 h, activity in the SARS-CoV-2 hamster model, and C_{max} above IC_{50} in a hamster PD experiment (Table 1). It was not possible to conduct comprehensive PK/PD analyses because additional efficacy data in hamsters would have been needed. Efficacious dosing regimens significantly reducing the lung $TCID_{50}$ in comparison to untreated control animals are illustrated in the Supplementary Materials (Figures S35–S46). Data generated here could not be used to derive the likely PD driver to achieve efficacy in the hamsters even though time above a minimum inhibitory concentration, total exposure, or C_{max} are all important parameters. A parallel with humans could be made, as when C_{max} exceeds the IC_{50} , clinical efficacy was also observed (evident for molnupiravir but not favipiravir) [49–51]. Each of these three

PK/PD parameters (exposure in hamsters above IC_{50} for 24 h, activity in the SARS-CoV-2 hamster model, and C_{max} above IC_{50} in the hamster PD experiment) was achieved only for nirmatrelvir. Regarding daclatasvir, ritonavir-boosted atazanavir, and sofosbuvir, none of the exposure targets was reached, and no activity was observed in hamsters.

3.3. Preclinical Data Generated for IAAs

From the IAA compounds selected for profiling, only clofazimine, colchicine, and ivermectin demonstrated some potency in all three in vitro cellular assays. However, potency of these compounds was associated with cell toxicity or a very low selectivity index (SI). Amodiaquine, cepharanthine, fluoxetine, and mefloquine (in addition to the abovementioned compounds) showed activity in the Vero cell line but no activity in Calu-3 or A549 cells (Table 1). Moreover, high potency ($<10 \mu\text{M}$) in Vero cells was associated with toxicity for most compounds with the exception of nitazoxanide. Nitazoxanide also showed high potency and no toxicity in Calu-3 cells, similar to camostat. All remaining IAA compounds (ambroxol, fluvoxamine, pentoxyfilline, probenecid, and proxalutamide) showed no potency in all three investigated cell lines (Table 1 and Table S5).

Regarding the ex vivo 3D model, only camostat mesylate and nitazoxanide showed activity in the primary HAE cells ($10 \mu\text{M}$ and $5 \mu\text{M}$, respectively) (Supplementary Materials Table S6).

With respect to drug exposure in humans at a clinically relevant dose, none of the IAA compounds reached exposure targets (Table 1 and Supplementary Materials Figures S20–S34). Likewise, C_{max} for the dosing regimens in hamsters matching human exposure failed to reach in vitro IC_{50} values corrected for protein binding. At doses tested in hamster efficacy experiments, simulated plasma exposures were below target concentrations. Clofazimine was the only exception (simulated C_{max} was above IC_{50} at 25 mg/kg). None of the IAA compounds demonstrated efficacy in in vivo hamster models (Table 1).

3.4. Preclinical Data Generated for Drug Combinations

As discussed, the project involved ongoing review of promising drug combinations based on newly generated preclinical and proof-of-concept clinical data. However, none of the combinations tested in vivo in the SARS-CoV-2 infection hamster model showed additive or synergistic efficacy (Table 2) above that reported for single compounds already shown to be efficacious in this model. The combination of favipiravir with nitazoxanide or atazanavir did not show any additive or synergistic activity compared with favipiravir alone. Similarly, the combination of clofazimine with molnupiravir did not show any additive or synergistic activity compared with molnupiravir alone. Interestingly, combining the two DAAs molnupiravir and nirmatrelvir—currently the only two drugs having received emergency use authorization from the FDA—did not lead to additive or synergistic efficacy at the doses tested (preliminary data).

4. Discussion and Lessons Learned

4.1. Selection of Repurposed Drugs

The selected repurposed drugs were chosen based on existing preclinical data and included, among others, known antivirals, antimalarials, antiparasitics, and host modulators (Supplementary Materials Table S4). While the initial selection of repurposed drugs for COVID-19 has concentrated on registered drugs originally developed for treatment against other viruses (e.g., HCV, HIV) and acting against known targets of the virus cycle (e.g., inhibitors of nsp13 helicase, inhibitors of RNA-dependent RNA polymerase [RdRp]), this did not necessarily prove to be a criterion for preclinical and in some cases clinical activity against SARS-CoV-2 (e.g., atazanavir, sofosbuvir). Indeed, the target sequence might differ or be less relevant due to differences between virus families [52].

Similarly, selection based on in vitro potency (possibly with an inadequate assay in Vero cells) and exposure in the relevant organs was also no guarantee of in vivo efficacy (e.g., clofazimine, atazanavir). In addition, drug exposure measurements observed for standard regimens in humans are not always achieved in the animal model for virus-induced disease,

making it complicated to postulate any potential efficacy or to assign a rationale for these drugs from a preclinical point of view. Indeed, hamsters tended to have much higher clearance rates for the drug than that seen in humans, and more frequent dosing than BID is extremely difficult under containment level 3/biosafety level 3 (CL-3/BSL-3) conditions.

4.2. Relevance of In Vitro Assays

Over the course of our study, and throughout the COVID-19 pandemic, a lack of standardized assays specially dedicated for SARS-CoV-2 was apparent, as has been reported by other laboratories [53,54]. In vitro assays do not always reflect the potential metabolism or required activation mechanism of the drug for it to show efficacy, hence the importance of knowing and understanding the drug's underlying mechanism of action.

Immortalized cell lines such as Vero cells offer a readily available system for initial screens. However, as steps of the viral replication cycle might be fundamentally altered in these cell lines, the risk of false positives (such as chloroquine [55]) and false negatives (such as camostat mesylate [56]) is high with in vitro assays. Meaningful counter screens must be integrated into any discovery campaign to validate the physiological relevance of results, for instance by using disease-relevant primary cells or organoid models [57], even though one cannot rule out that other cell systems could also result in false positives or false negatives.

Published in vitro potency data in cell systems have shown that atazanavir (ATZ) and the ATZ/ritonavir combination are active against the SARS-CoV-2 virus [58]. Consistent EC₅₀ values of 0.5–9.4 µM and 0.6 µM have been reported in SARS-CoV-2-infected Vero cells and infected A549 lung epithelia cells, respectively [58,59]. However, the choice of host cell used for testing in vitro potency of selected repurposed compounds may have an impact on the assay itself. One of the major limitations of Vero cells is that they are defective in the expression of the main SARS-CoV-2 receptors (angiotensin-converting enzyme 2/ACE2 and transmembrane protease serine 2/TMPRSS2) known to play a pivotal role in SARS-CoV-2 binding and cell entry [60]. In addition, Vero cells express the functionally active P-glycoprotein (Pgp) efflux pump, which could be a source of bias for in vitro studies of drugs with Pgp-mediated drug transport [61]. Moreover, phospholipidosis in Vero cells has been shown for ex vivo cationic amphiphilic drug to correlate with an absence of in vivo success so far, suggesting that relying on this sole MoA would translate into a lack of clinical efficacy of most drugs repurposed to date for SARS-CoV-2. Hence, distinguishing compounds with this confounding effect could accelerate the identification of genuinely potent antivirals against SARS-CoV-2 and other viruses [62].

Human airway epithelial Calu-3 cells were used to understand the pathophysiology of the virus, as they also express the TMPRSS2 receptors. They were shown to be permissive to many coronaviruses, including SARS-CoV-2, and were described as a suitable host cell line that allows the virus to grow in vitro despite a low throughput. Rapidly, the use of lung epithelial cells showed differences in drug sensitivities compared to Vero cells (e.g., hydroxychloroquine versus remdesivir, as described by Dittmar and colleagues [63]). Further studies have demonstrated that ACE2 and TMPRSS2 receptors were expressed in lungs and in bronchial transient secretory cells [64], strongly supporting the importance of using tissue-relevant cell lines to profile any drugs in vitro against the SARS-CoV-2 virus.

Possibly the most relevant and predictive cell line for in vitro potency assays was the A549-TMPRSS2 adenocarcinoma human alveolar basal epithelial cell line, whose receptors are closely related to respiratory cells; SARS-CoV-2 uses the SARS-CoV receptor ACE2 for host cell entry [64,65]. In our experience, A549 airway epithelial cells were the most reliable for in vitro/in vivo translation purposes, with the exception of favipiravir, which did not show any in vitro activity. This drug was, however, used as calibrator for in vivo models as it was the only efficacious drug in the PD models available at the beginning of the pandemic. The example of favipiravir highlights a major limitation observed in the translation of in vitro to in vivo data when it comes to compounds having a complex in vivo metabolism. Similarly, we were unable to reproduce potency data for the bemnifosbuvir

(AT-527) experimental compound, which was tested in a Phase 2 trial but failed to meet the primary end point of reduction from baseline in the amount of SARS-CoV-2 virus in patients with mild or moderate COVID-19 compared to placebo [66].

Another ex vivo/in vitro cell model of the human airway epithelium cultured at the air–liquid interface emerged during the pandemic and was widely used. The use of this 3D model demonstrated good prediction of positive efficacy outcome in the PD hamster model with the same exception as above. Favipiravir did not show any ex vivo activity, while being efficacious in the in vivo hamster model; conversely, nelfinavir and nitazoxanide only demonstrated ex vivo potency at high concentration but no in vivo efficacy.

Whenever possible, we highly recommend that drugs be assessed on multiple in vitro potency assays to avoid any confounding factors and to add confidence to the translatability of in vitro data. A drug that demonstrates the same range of IC_{50} on multiple cell lines has a higher potential to show in vivo efficacy if adequate exposure can be reached. Confirmation of in vitro data in several laboratories using the same assay will also build confidence in moving a drug to the next stage, be it in vivo animal models or clinical PoC.

The current analysis reveals that many potential drugs are unlikely to achieve the human target concentrations necessary to adequately suppress SARS-CoV-2 under normal dosing conditions. The data emerging from global screening efforts were not routinely benchmarked and prioritized against achievable concentrations after administration of doses proven to have acceptable safety profiles in humans [30].

Of the many treatment options tested preclinically and clinically, the majority of reports of in vitro activity focused on EC_{50} and did not consider $EC_{90/95}$ or protein-adjusted $EC_{90/95}$ as per antiviral convention [29,30], nor did they consider the achievable concentrations in plasma or relevant compartments such as lungs for COVID-19. EC_{50} alone in plasma may not be a strong enough indicator of antiviral activity. It is critical that candidate medicines emerging from in vitro antiviral screening programs are considered in the context of their expected exposure in humans where possible. Lung accumulation in addition to plasma exposure could provide additional insights regarding therapeutic advantage and reassurance to move forward to clinical trials [30]. However, given the different tropism in newly emerging variants of SARS-CoV-2 such as the Omicron variant sub-lineages, the lung is becoming less relevant as a specific target organ in which antiviral exposure should exceed EC_{90} of the drug.

4.3. Relevance of In Vivo Assays

Among the limitations of the repurposing approach is the formulation of the active pharmaceutical ingredient (API) for in vivo study in animal models, since these are often not available in formulations or possible volumes of administration that would exert an adequate exposure in hamster disease models [67]. Moreover, the mode of administration of the drug such as infusion or inhalation can make its assessment especially difficult in BSL-3 laboratories.

Current animal models are limited to the detection of direct antiviral activity. As such, the host-directed effect is not captured. However, one could argue that in some instances, while looking at other readouts, in particular inflammation using histology methods or measuring cytokine release, some positive effects related to disease outcome can be detected, with their relevance yet to be confirmed clinically. Nelfinavir, for example, provided a measure of clinical efficacy by reducing lung inflammation in the hamster model of infection, although no effect on viral load was observed [46]. Our experience showed that there is a need for a clear definition of the targeted stage of the disease, as antivirals are likely indicated in the early disease stage to reduce the viral load, whereas anti-inflammatory drugs are required in late-stage disease to address the cytokine storm or other symptoms emerging from COVID-19 disease. As there is no adequate model to assess anti-inflammatory symptoms and consequences of viral infection, the repurposing approach described focused mainly on the antiviral efficacy of compounds, which represents only part of the approach needed to combat COVID-19. Indeed, depending on patient needs and risks,

management of COVID-19 can involve intensive care, oxygen therapy, anticoagulation therapy, steroids, antivirals, or immunomodulation drugs [68]. From a public health perspective, appropriately selected and tested repurposed antiviral drugs can relieve the burden of hospitalizations, but they are not the only available tools against COVID-19.

Our study suggested that it would be beneficial for SARS-CoV-2 activity data to be performed with standardized protocols and with standardized effective concentration (EC) activity values as a marker of the concentrations required to suppress the virus to therapeutically relevant levels [30]. Our investigations highlighted a lack of preclinical data on antiviral efficacy in relevant *in vivo* models compared to relevant benchmarks (e.g., remdesivir, favipiravir) [38,69]. Drugs for which IC_{50} is not reached by C_{max} or C_{min} also showed no activity in the PD hamster study. For those compounds that reached target exposures, activity in hamsters needed to be confirmed, i.e., simulation can detect true negative but not the true positive (Table 3).

Table 3. Target exposure vs. activity in the hamster infection model of SARS-CoV-2.

C_{max} in Hamster above Corrected IC_{50}	Activity in Hamster Infection Model of SARS-CoV-2		Total
	Yes	No	
Yes	TRUE POSITIVE (TP) $n = 3$ (favipiravir, molnupiravir, nirmatrelvir)	FALSE POSITIVE (FP) $n = 1$ (clofazimine)	4
No	FALSE NEGATIVE (FN) $n = 0$	TRUE NEGATIVE (TN) $n = 12$ (atazanavir, bemnifosbuvir, daclatasvir, nelfinavir *, sofosbuvir, ambroxol, amodiaquine, cepharanthine, fluoxetine, fluvoxamine, ivermectin, nitazoxanide)	12
Total	3	13	16

* no effect on viral load was detected, but a diminution of lung inflammation and “disease” outcome was nevertheless observed; sensitivity: 100% (TP/TP + FN); specificity: 92% (TN/FP + TN).

Population PK simulations help suggest relevant preclinical dosing regimens and understand the dose–response relationship. When added to available information regarding safety, availability, and cost, these data played a critical role in the overall assessment of the suitability of possible repurposed treatments. For several compounds (daclatasvir, colchicine, fluvoxamine maleate, mefloquine, and nitazoxanide), our experiments showed that it was not possible to achieve a plasma concentration exceeding a relevant *in vitro* EC_{50} against SARS-CoV-2 for 24 h, taking into consideration plasma protein binding. This criterion was, however, achieved with nirmatrelvir, which showed a significant reduction of the lung $TCID_{50}$ of SARS-CoV-2 in the hamster model. It is important to note that for the simulations performed, we assumed that the (unbound) free drug hypothesis holds [29].

Interestingly, population PK modeling and simulations performed for bemnifosbuvir (AT-527) experimental drug showed that the IC_{50} reported in the literature [70] was not reached in hamsters at any of the doses tested. This result correlates with a lack of efficacy since no activity in the PD hamster study could be observed.

Another important aspect concerning COVID-19 is the management of patients developing severe or critical disease. For those patients, antiviral therapies are insufficient and must be complemented with corticosteroids, immunomodulators, and supplemental oxygen. The preclinical models described above are not suited to identify such treatments or to make therapeutic recommendations based on disease severity for the management of hospitalized COVID-19 patients.

4.4. Working under Time Pressure

Over the course of the COVID-19 pandemic, the scientific community has been called to rise to the occasion with unprecedented intensity and urgency [71]. While growing im-

munity and the availability of vaccines and first generation DAAs in high income countries has changed the current COVID landscape (even though new virus variants with additional capacity to escape the immune response continue to emerge), we can begin to reflect on the triumphs and challenges related to drug repurposing. In addition to a number of clinical trials not being initially well-suited to a public health emergency, some trials initiated in the early days of the pandemic were underpowered and poorly designed, leading to wasted resources generating false leads as seen in the enthusiastic but ultimately refuted reaction to hydroxychloroquine or ivermectin [72]. Because of the urgency to identify clinical candidates, decisions were made using data generated on existing and available assays (such as in vitro activity assays in Vero cells, as explained above). Additional examples of false leads include sofosbuvir/daclatasvir, lopinavir/ritonavir, and chloroquine that all showed negative results or no effect in clinical trials [73–75], while questionable validity of preclinical evidence for atazanavir [58] and amodiaquine [76] still needs robust clinical assessment before completely discarding these two drugs.

The challenges of fast developing treatment strategies were unprecedented during COVID-19. During the pandemic, research in the field was churned out at an unprecedented speed and was complicated by a steady appearance of new variants of concern [77]. Indeed, the SARS-CoV-2 variants used in vivo do not show the same cellular tropism as the current ones (e.g., Omicron sub-lineages). A key issue is that the variants have been emerging faster than the time required for producing data for relevant drugs. Similarly, from a logistical point of view, there is no way of fast-tracking animal models. It takes time to develop specifically dedicated models both in vitro and in vivo. Researchers were confronted with balancing urgency of response versus rational scientific decision while integrating growing knowledge of the disease.

In an effort to be collaborative and transparent, a wealth of data was shared on open access platforms, which was an invaluable contribution to the scientific community. In some instances, again because of the speed of reaction, this fair approach also included making preliminary data (not peer reviewed) accessible that did not always justify the further development of identified drugs. Other clear limitations shown during our study and highlighted above remain the identification of potential drugs of interest having an MoA other than antiviral activity. Achieving clinically relevant exposure in animal models was an additional challenge for the identification of adequate repurposed drugs for the treatment of COVID-19, related among others to the need for optimal formulation and different metabolism in animal species.

5. Conclusions

Despite remarkable collaborative efforts, the scientific community lacks standardized preclinical procedures and data packages that can help inform drug choice. We noted that preclinical information at times provided conflicting evidence compared with antiviral activity described in the literature, emphasizing the need for a standardized preclinical data package to better inform evidence-based decision making and later clinical development. For example, a partnership has identified a gap in existing clinical trial pipelines that merits investment in further evidence generation for repurposed antivirals and combinations regimens [78]. This highlights the challenges involved in rapidly identifying antiviral treatments and the need for an improved and standardized drug development process. A unified standardized strategy is necessary for selecting, testing, and validating candidate drugs.

Repurposing drugs for COVID-19 has been limited by an empirical choice based on limited data and often following sparse data from in vitro assays without a strong rationale. As stated by Grobler et al. [53], there is a need for a coordinated systematic approach to identify and test promising drugs. Since repurposed drugs were not optimized for the treatment of COVID-19, clearly defined and harmonized criteria from preclinical data must be implemented to be better prepared and to respond faster in the event of a new pandemic. The necessary short-term dependence on repurposing existing drugs cannot be relied upon

to produce true successful outcomes. For the future, we should begin to work on potent oral antivirals against all major classes of potential pathogens, with the goal of having drugs ready for Phase 2/3 efficacy trials when the next threat emerges.

Our collaboration identified key drug repurposing opportunities for COVID-19 treatment and prevention and highlighted the importance of standardized testing of preclinical data such as PK exposure when interpreting the emerging candidacy of drugs for COVID-19 treatment and prevention. Overall, we believe that following the standardized process to assess repurposed drugs described in Figure 1, we could improve translation of selected repurposed compounds to clinical trials. It is interesting to note that the current WHO guidelines and recommendations for the use of given drugs [79] reflect our observations, in that nirmatrelvir and molnupiravir are recommended for COVID-19 treatment, whereas ivermectin, hydroxychloroquine, and lopinavir/ritonavir are not recommended. Further drugs will be added to the list once robust clinical data are available.

We advocate a multi-pronged approach to drug repurposing for COVID-19 treatment, using the preclinical tests presented in the current study, including carrying out the same assay in different laboratories across different cell lines. This pragmatic approach is intended to build confidence in the validity of preclinical data. No one model fits all, but several strategies are required depending on the MoA of the drug.

Identification of efficacious drugs against COVID-19 will reduce viral load in patients, reduce hospitalizations, and ultimately relieve healthcare systems. Sobering data from the WHO point to the impact of the pandemic and to the need for countries to invest in more resilient health systems that can sustain essential health services during crises, including stronger health information systems [5]. The lessons learned will be critical in improving the response and control of future pandemics.

Supplementary Materials: The following supporting information can be downloaded at: <https://www.mdpi.com/article/10.3390/microorganisms10081639/s1>, Section S1: Experimental details; Section S2: Results; Table S1: Experimental conditions for in vivo efficacy studies in SARS-CoV-2 hamster models; Table S2: Experimental conditions for pharmacokinetic studies in female Golden Syrian hamsters; Table S3: Bioanalytical conditions for pharmacokinetic studies in hamsters; Table S4: Summary of literature data for prioritized compounds selected for preclinical assessments; Table S5: Summary of generated in vitro data for prioritized compounds selected for preclinical assessments; Table S6: Summary of generated ex vivo data for prioritized compounds selected for preclinical assessments; Table S7: Protein binding and in vitro activity for repurposed drug candidates; Table S8: Overview of pharmacokinetic models in hamsters and humans; Table S9–S27: Pharmacokinetic parameters for each drug (hamsters and humans); Table S28: Exposure in humans at clinical dose and doses in hamsters matching human pharmacokinetic parameters; Figures S1–S17: In vivo pharmacokinetic profile for each drug following administration to Syrian golden hamsters; Figure S18: Graphical representation of a 2-compartment disposition model; Figure S19: Graphical representation of a 1-compartment disposition model for both parent and metabolite; Figures S20–S34: Simulated pharmacokinetic parameters in humans and hamsters for each drug; Figures S35–S46: In vivo efficacy for each drug in the SARS-CoV-2 hamster model. References can be seen [80–151].

Author Contributions: Conceptualization, R.A., A.N., D.J., L.F., C.E.M., A.O., R.M.H., J.T., P.S., F.E., I.S. and E.C.; methodology, F.A., J.-S.D., R.A., L.V., F.T., A.A., M.C., P.C., D.J., L.L., T.W., R.M.H., J.T. and A.N.; software, F.A., A.A., P.C. and T.W.; validation, F.A., J.-S.D., R.A., L.V., F.T., A.A., P.C. and T.W.; formal analysis, F.A., J.-S.D., R.A., L.V., F.T., A.A., P.C., M.C., C.S.F., D.J., S.K., L.L., G.M., S.P., P.-R.P., T.W., B.W., R.M.H., J.T., F.E., I.S. and E.C.; investigation, J.-S.D., R.A., L.V., F.T., M.C., C.S.F., D.J., S.K., L.L., G.M., S.P., P.-R.P., B.W. and A.N.; data curation, F.A., J.-S.D., R.A., L.V., F.T., A.A., P.C. and T.W.; writing—original draft preparation: F.A., P.S., F.E., I.S. and E.C.; writing—review and editing, F.A., J.-S.D., R.A., F.T., A.A., P.C., D.J., D.S., T.W., J.-R.I., A.O., R.M.H., J.T., A.N., P.S., F.E., I.S. and E.C.; visualization, F.A., J.-S.D., R.A., L.V., F.T., A.A., P.C., C.S.F., D.J., T.W., F.E., I.S. and E.C.; supervision, J.N., X.d.L., A.N., D.S., F.T., R.M.H., J.T., F.E., I.S. and E.C.; project administration, J.-S.D., L.V., C.S.F., F.T., D.S., J.-R.I., F.E., I.S. and E.C.; funding acquisition, L.F., C.E.M., J.T., J.N., X.d.L., A.O., F.E., I.S. and E.C. All authors have read and agreed to the published version of the manuscript.

Funding: This project was carried out and funded through DNDi under the support by the Wellcome Trust Grant ref: 222489/Z/21/Z through the “COVID-19 Therapeutics Accelerator”. For part of this work, DNDi received also funding from the Federal Ministry of Education and Research (BMBF) through KfW (Germany) and the Foreign Commonwealth & Development Office (FCDO, UK). AO acknowledges funding by Wellcome Trust (222489/Z/21/Z), EPSRC (EP/R024804/1; EP/S012265/1), NIH (R01AI134091; R24AI118397) and Unitaid (2020-38-LONGEVITY). For the purpose of open access, the author has applied a CC-BY public copyright licence to any author-accepted manuscript version arising from this submission.

Institutional Review Board Statement: Housing conditions and experimental procedures for animal studies were approved by: the ethics committee of animal experimentation of KU Leuven (license P065-2020) for studies performed at KU Leuven; the ethical committee of Marseille (C2EA—14) and the French ‘Ministère de l’Enseignement Supérieur, de la Recherche et de l’Innovation’ (APAFIS#23975) for studies performed at UVE, Marseille.

Informed Consent Statement: Not applicable.

Data Availability Statement: Not applicable.

Acknowledgments: We thank Vanessa Gray-Schopfer, OmniScience SA (manuscript) for providing medical writing support funded by DNDi. We thank Camille Placidi (Unité des Virus Emergents, Marseille, France) for her technical contribution. We thank Caroline Laprie (Laboratoire Vet-Histo, Marseille, France) for the histological analysis. The authors were fully responsible for contents and editorial decisions for this report.

Conflicts of Interest: The authors declare no conflict of interest. The funders had no role in the design of the study; in the collection, analyses, or interpretation of data; in the writing of the manuscript; or in the decision to publish the results. AO is Director of Tandem Nano Ltd. and co-inventor of patents relating to drug delivery. AO has received research funding from ViiV, Merck, Janssen and consultancy from Gilead, ViiV and Merck not related to the current paper.

References

1. Valencia, D.N. Brief Review on COVID-19: The 2020 Pandemic Caused by SARS-CoV-2. *Cureus* **2020**, *12*, e7386. [CrossRef]
2. WHO Director-General’s Opening Remarks at the Media Briefing on COVID-19. 11 March 2020. Available online: <https://www.who.int/director-general/speeches/detail/who-director-general-s-opening-remarks-at-the-media-briefing-on-covid-19--11-march-2020> (accessed on 14 April 2022).
3. WHO Coronavirus (COVID-19) Dashboard. Available online: <https://covid19.who.int/> (accessed on 15 June 2022).
4. COVID-19 Dashboard by the Center for Systems Science and Engineering (CSSE) at Johns Hopkins University (JHU). Available online: <https://coronavirus.jhu.edu/map.html> (accessed on 14 April 2022).
5. World Health Organization. Press Release. 14.9 Million Excess Deaths Associated with the COVID-19 Pandemic in 2020 and 2021. Available online: <https://www.who.int/news/item/05-05-2022-14.9-million-excess-deaths-were-associated-with-the-covid-19-pandemic-in-2020-and-2021> (accessed on 5 May 2022).
6. Wang, D.; Hu, B.; Hu, C.; Zhu, F.; Liu, X.; Zhang, J.; Wang, B.; Xiang, H.; Cheng, Z.; Xiong, Y.; et al. Clinical Characteristics of 138 Hospitalized Patients With 2019 Novel Coronavirus-Infected Pneumonia in Wuhan, China. *JAMA* **2020**, *323*, 1061–1069. [CrossRef]
7. Schultze, J.L.; Aschenbrenner, A.C. COVID-19 and the human innate immune system. *Cell* **2021**, *184*, 1671–1692. [CrossRef]
8. Hu, B.; Guo, H.; Zhou, P.; Shi, Z.L. Characteristics of SARS-CoV-2 and COVID-19. *Nat. Rev. Microbiol.* **2021**, *19*, 141–154. [CrossRef]
9. COVID-19 Clinical Research Coalition. Available online: <https://covid19crc.org/> (accessed on 14 April 2022).
10. ANTICOV Consortium. ANTICOV Clinical Trial. Available online: <https://anticov.org/> (accessed on 5 May 2022).
11. Tobinick, E.L. The value of drug repositioning in the current pharmaceutical market. *Drug News Perspect.* **2009**, *22*, 119–125. [CrossRef] [PubMed]
12. Sleight, S.H.; Barton, C.L. Repurposing Strategies for Therapeutics. *Pharm. Med.* **2010**, *24*, 151–159. [CrossRef]
13. Chavda, V.P.; Kapadia, C.; Soni, S.; Prajapati, R.; Chauhan, S.C.; Yallapu, M.M.; Apostolopoulos, V. A global picture: Therapeutic perspectives for COVID-19. *Immunotherapy* **2022**, *14*, 351–371. [CrossRef]
14. Novac, N. Challenges and opportunities of drug repositioning. *Trends Pharmacol. Sci.* **2013**, *34*, 267–272. [CrossRef]
15. Sultana, J.; Crisafulli, S.; Gabbay, F.; Lynn, E.; Shakir, S.; Trifiro, G. Challenges for Drug Repurposing in the COVID-19 Pandemic Era. *Front. Pharmacol.* **2020**, *11*, 588654. [CrossRef]
16. Chen, B.; Tian, E.K.; He, B.; Tian, L.; Han, R.; Wang, S.; Xiang, Q.; Zhang, S.; El Arnaout, T.; Cheng, W. Overview of lethal human coronaviruses. *Signal Transduct. Target, Ther.* **2020**, *5*, 89. [CrossRef]

17. Mercorelli, B.; Palù, G.; Loregian, A. Drug Repurposing for Viral Infectious Diseases: How Far Are We? *Trends Microbiol.* **2018**, *26*, 865–876. [CrossRef] [PubMed]
18. Kim, W.Y.; Kweon, O.J.; Cha, M.J.; Baek, M.S.; Choi, S.H. Dexamethasone may improve severe COVID-19 via ameliorating endothelial injury and inflammation: A preliminary pilot study. *PLoS ONE* **2021**, *16*, e0254167. [CrossRef] [PubMed]
19. Ledford, H. Coronavirus breakthrough: Dexamethasone is first drug shown to save lives. *Nature* **2020**, *582*, 469. [CrossRef]
20. Mahase, E. COVID-19: Anti-inflammatory treatment baricitinib reduces deaths in patients admitted to hospital, finds trial. *BMJ* **2022**, *376*, o573. [CrossRef]
21. Lawler, P.R.; Goligher, E.C.; Berger, J.S.; Neal, M.D.; McVerry, B.J.; Nicolau, J.C.; Gong, M.N.; Carrier, M.; Rosenson, R.S.; Reynolds, H.R.; et al. Therapeutic Anticoagulation with Heparin in Noncritically Ill Patients with Covid-19. *N. Engl. J. Med.* **2021**, *385*, 790–802. [CrossRef]
22. Barnes, G.D.; Burnett, A.; Allen, A.; Ansell, J.; Blumenstein, M.; Clark, N.P.; Crowther, M.; Dager, W.E.; Deitelzweig, S.B.; Ellsworth, S.; et al. Thromboembolic prevention and anticoagulant therapy during the COVID-19 pandemic: Updated clinical guidance from the anticoagulation forum. *J. Thromb. Thrombolysis* **2022**, *54*, 197–210. [CrossRef]
23. National Institutes of Health COVID-19 Treatment Guidelines. Antithrombotic Therapy in Patients with COVID-19. Available online: <https://www.covid19treatmentguidelines.nih.gov/therapies/antithrombotic-therapy/> (accessed on 2 August 2022).
24. Rannard, S.P.; McDonald, T.O.; Owen, A. Chasing COVID-19 chemotherapeutics without putting the cart before the horse. *Br. J. Clin. Pharmacol.* **2020**. [CrossRef]
25. Bayat Mokhtari, R.; Homayouni, T.S.; Baluch, N.; Morgatskaya, E.; Kumar, S.; Das, B.; Yeager, H. Combination therapy in combating cancer. *Oncotarget* **2017**, *8*, 38022–38043. [CrossRef]
26. Shyr, Z.A.; Cheng, Y.S.; Lo, D.C.; Zheng, W. Drug combination therapy for emerging viral diseases. *Drug Discov. Today* **2021**, *26*, 2367–2376. [CrossRef]
27. Akinbolade, S.; Coughlan, D.; Fairbairn, R.; McConkey, G.; Powell, H.; Ogunbayo, D.; Craig, D. Combination therapies for COVID-19: An overview of the clinical trials landscape. *Br. J. Clin. Pharmacol.* **2022**, *88*, 1590–1597. [CrossRef]
28. Pushpakom, S.; Iorio, F.; Eyers, P.A.; Escott, K.J.; Hopper, S.; Wells, A.; Doig, A.; Guilliams, T.; Latimer, J.; McNamee, C.; et al. Drug repurposing: Progress, challenges and recommendations. *Nat. Rev. Drug Discov.* **2019**, *18*, 41–58. [CrossRef] [PubMed]
29. Boffito, M.; Back, D.J.; Flexner, C.; Sjö, P.; Blaschke, T.F.; Horby, P.W.; Cattaneo, D.; Acosta, E.P.; Anderson, P.; Owen, A. Toward Consensus on Correct Interpretation of Protein Binding in Plasma and Other Biological Matrices for COVID-19 Therapeutic Development. *Clin. Pharmacol. Ther.* **2021**, *110*, 64–68. [CrossRef] [PubMed]
30. Arshad, U.; Pertinez, H.; Box, H.; Tatham, L.; Rajoli, R.K.R.; Curley, P.; Neary, M.; Sharp, J.; Liptrott, N.J.; Valentijn, A.; et al. Prioritization of Anti-SARS-Cov-2 Drug Repurposing Opportunities Based on Plasma and Target Site Concentrations Derived from their Established Human Pharmacokinetics. *Clin. Pharmacol. Ther.* **2020**, *108*, 775–790. [CrossRef] [PubMed]
31. Eugene, A.R. Fluoxetine pharmacokinetics and tissue distribution quantitatively supports a therapeutic role in COVID-19 at a minimum dose of 20 mg per day. *F1000Research* **2022**, *10*, 477. [CrossRef]
32. Ivens, T.; Van den Eynde, C.; Van Acker, K.; Nijs, E.; Dams, G.; Bettens, E.; Ohagen, A.; Pauwels, R.; Hertogs, K. Development of a homogeneous screening assay for automated detection of antiviral agents active against severe acute respiratory syndrome-associated coronavirus. *J. Virol. Methods* **2005**, *129*, 56–63. [CrossRef]
33. Do, T.N.D.; Donckers, K.; Vangeel, L.; Chatterjee, A.K.; Gallay, P.A.; Bobardt, M.D.; Bilello, J.P.; Cihlar, T.; De Jonghe, S.; Neyts, J.; et al. A robust SARS-CoV-2 replication model in primary human epithelial cells at the air liquid interface to assess antiviral agents. *Antivir. Res.* **2021**, *192*, 105122. [CrossRef]
34. Drugs for Neglected Diseases Initiative. Target Product Profile for COVID-19. Available online: <https://dndi.org/diseases/covid-19/target-product-profile/> (accessed on 15 June 2022).
35. Abdelnabi, R.; Foo, C.S.; Jochmans, D.; Vangeel, L.; De Jonghe, S.; Augustijns, P.; Mols, R.; Weynand, B.; Wattanakul, T.; Høglund, R.M.; et al. The oral protease inhibitor (PF-07321332) protects Syrian hamsters against infection with SARS-CoV-2 variants of concern. *Nat. Commun.* **2022**, *13*, 719. [CrossRef]
36. Boudewijns, R.; Thibaut, H.J.; Kaptein, S.J.F.; Li, R.; Vergote, V.; Seldeslachts, L.; Van Weyenbergh, J.; De Keyzer, C.; Bervoets, L.; Sharma, S.; et al. STAT2 signaling restricts viral dissemination but drives severe pneumonia in SARS-CoV-2 infected hamsters. *Nat. Commun.* **2020**, *11*, 5838. [CrossRef]
37. Kaptein, S.J.F.; Jacobs, S.; Langendries, L.; Seldeslachts, L.; Ter Horst, S.; Liesenborghs, L.; Hens, B.; Vergote, V.; Heylen, E.; Barthelémy, K.; et al. Favipiravir at high doses has potent antiviral activity in SARS-CoV-2-infected hamsters, whereas hydroxychloroquine lacks activity. *Proc. Natl. Acad. Sci. USA* **2020**, *117*, 26955–26965. [CrossRef]
38. Driouich, J.S.; Cochin, M.; Lingas, G.; Moureau, G.; Touret, F.; Petit, P.R.; Piorkowski, G.; Barthelémy, K.; Laprie, C.; Coutard, B.; et al. Favipiravir antiviral efficacy against SARS-CoV-2 in a hamster model. *Nat. Commun.* **2021**, *12*, 1735. [CrossRef]
39. Wattanakul, T.; Chotsiri, P.; Scandale, I.; Høglund, R.M.; Tarning, J. Pharmacometric approach to evaluate drug for potential repurposing as COVID-19 therapeutics. *Expert Rev. Clin. Pharmacol.* **2022**; submitted.
40. Lavielle, M. mlxR: Simulation of Longitudinal Data. R Package Version 4.2.0. 2021. Available online: <https://cran.r-project.org/web/packages/mlxR/index.html> (accessed on 15 June 2022).
41. Clemency, B.M.; Varughese, R.; Gonzalez-Rojas, Y.; Morse, C.G.; Phipatanakul, W.; Koster, D.J.; Blaiss, M.S. Efficacy of Inhaled Ciclesonide for Outpatient Treatment of Adolescents and Adults With Symptomatic COVID-19: A Randomized Clinical Trial. *JAMA Intern. Med.* **2022**, *182*, 42–49. [CrossRef] [PubMed]

42. Ramakrishnan, S.; Nicolau, D.V., Jr.; Langford, B.; Mahdi, M.; Jeffers, H.; Mwasuku, C.; Krassowska, K.; Fox, R.; Binnian, I.; Glover, V.; et al. Inhaled budesonide in the treatment of early COVID-19 (STOIC): A phase 2, open-label, randomised controlled trial. *Lancet Respir. Med.* **2021**, *9*, 763–772. [[CrossRef](#)]
43. Yu, L.M.; Bafadhel, M.; Dorward, J.; Hayward, G.; Saville, B.R.; Gbinigie, O.; Van Hecke, O.; Ogburn, E.; Evans, P.H.; Thomas, N.P.B.; et al. Inhaled budesonide for COVID-19 in people at high risk of complications in the community in the UK (PRINCIPLE): A randomised, controlled, open-label, adaptive platform trial. *Lancet* **2021**, *398*, 843–855. [[CrossRef](#)]
44. Si, L.; Bai, H.; Rodas, M.; Cao, W.; Oh, C.Y.; Jiang, A.; Moller, R.; Hoagland, D.; Oishi, K.; Horiuchi, S.; et al. A human-airway-on-a-chip for the rapid identification of candidate antiviral therapeutics and prophylactics. *Nat. Biomed. Eng.* **2021**, *5*, 815–829. [[CrossRef](#)] [[PubMed](#)]
45. Ohashi, H.; Watashi, K.; Saso, W.; Shionoya, K.; Iwanami, S.; Hirokawa, T.; Shirai, T.; Kanaya, S.; Ito, Y.; Kim, K.S.; et al. Potential anti-COVID-19 agents, cepharanthine and nelfinavir, and their usage for combination treatment. *iScience* **2021**, *24*, 102367. [[CrossRef](#)]
46. Foo, C.S.; Abdelnabi, R.; Kaptein, S.J.F.; Zhang, X.; Ter Horst, S.; Mols, R.; Delang, L.; Rocha-Pereira, J.; Coelmont, L.; Leyssen, P.; et al. HIV protease inhibitors Nelfinavir and Lopinavir/Ritonavir markedly improve lung pathology in SARS-CoV-2-infected Syrian hamsters despite lack of an antiviral effect. *Antivir. Res.* **2022**, *202*, 105311. [[CrossRef](#)]
47. Riccardi, N.; Giacomelli, A.; Canetti, D.; Comelli, A.; Intini, E.; Gaiera, G.; Diaw, M.M.; Udwardia, Z.; Besozzi, G.; Codecasa, L.; et al. Clofazimine: An old drug for never-ending diseases. *Future Microbiol.* **2020**, *15*, 557–566. [[CrossRef](#)]
48. Yuan, S.; Yin, X.; Meng, X.; Chan, J.F.; Ye, Z.W.; Riva, L.; Pache, L.; Chan, C.C.; Lai, P.M.; Chan, C.C.; et al. Clofazimine broadly inhibits coronaviruses including SARS-CoV-2. *Nature* **2021**, *593*, 418–423. [[CrossRef](#)]
49. Fujifilm Press Release. Anti-Influenza Drug Avigan® Tablet Meets Primary Endpoint in Phase III Clinical Trial in Japan for COVID-19 Patients. 23 September 2020. Available online: <https://www.fujifilm.com/jp/en/news/hq/5451> (accessed on 24 June 2022).
50. Merck Press Release. Merck and Ridgeback to Present Data Demonstrating That Treatment With LAGEVRIO™ (Molnupiravir) Was Associated with More Rapid Elimination of Infectious SARS-CoV-2 Than Placebo. 1 April 2022. Available online: <https://www.merck.com/news/merck-and-ridgeback-to-present-data-demonstrating-that-treatment-with-lagevrio-molnupiravir-was-associated-with-more-rapid-elimination-of-infectious-sars-cov-2-than-placebo/> (accessed on 24 June 2022).
51. Pfizer Press Release. Pfizer Announces Additional Phase 2/3 Study Results Confirming Robust Efficacy of Novel COVID-19 Oral Antiviral Treatment Candidate in Reducing Risk of Hospitalization or Death. 14 December 2021. Available online: <https://www.pfizer.com/news/press-release/press-release-detail/pfizer-announces-additional-phase-23-study-results> (accessed on 24 June 2022).
52. Burrell, C.J.; Howard, C.R.; Murphy, F.A. Classification of Viruses and Phylogenetic Relationships. *Fenner White's Med. Virol.* **2017**, 15–25. [[CrossRef](#)]
53. Grobler, J.A.; Anderson, A.S.; Fernandes, P.; Diamond, M.S.; Colvis, C.M.; Menetski, J.P.; Alvarez, R.M.; Young, J.A.T.; Carter, K.L. Accelerated Preclinical Paths to Support Rapid Development of COVID-19 Therapeutics. *Cell Host Microbe* **2020**, *28*, 638–645. [[CrossRef](#)]
54. Salasc, F.; Lahlali, T.; Laurent, E.; Rosa-Calatrava, M.; Pizzorno, A. Treatments for COVID-19: Lessons from 2020 and new therapeutic options. *Curr. Opin. Pharmacol.* **2022**, *62*, 43–59. [[CrossRef](#)] [[PubMed](#)]
55. Hoffmann, M.; Mosbauer, K.; Hofmann-Winkler, H.; Kaul, A.; Kleine-Weber, H.; Kruger, N.; Gassen, N.C.; Muller, M.A.; Drosten, C.; Pohlmann, S. Chloroquine does not inhibit infection of human lung cells with SARS-CoV-2. *Nature* **2020**, *585*, 588–590. [[CrossRef](#)] [[PubMed](#)]
56. Hoffmann, M.; Hofmann-Winkler, H.; Smith, J.C.; Krüger, N.; Arora, P.; Sørensen, L.K.; Søgaard, O.S.; Hasselstrøm, J.B.; Winkler, M.; Hempel, T.; et al. Camostat mesylate inhibits SARS-CoV-2 activation by TMPRSS2-related proteases and its metabolite GBPA exerts antiviral activity. *EBioMedicine* **2021**, *65*, 103255. [[CrossRef](#)] [[PubMed](#)]
57. Han, Y.; Duan, X.; Yang, L.; Nilsson-Payant, B.E.; Wang, P.; Duan, F.; Tang, X.; Yaron, T.M.; Zhang, T.; Uhl, S.; et al. Identification of SARS-CoV-2 inhibitors using lung and colonic organoids. *Nature* **2021**, *589*, 270–275. [[CrossRef](#)]
58. Fintelman-Rodrigues, N.; Sacramento, C.Q.; Ribeiro Lima, C.; Souza da Silva, F.; Ferreira, A.C.; Mattos, M.; de Freitas, C.S.; Cardoso Soares, V.; da Silva Gomes Dias, S.; Temerozo, J.R.; et al. Atazanavir, Alone or in Combination with Ritonavir, Inhibits SARS-CoV-2 Replication and Proinflammatory Cytokine Production. *Antimicrob. Agents Chemother.* **2020**, *64*, e00825-20. [[CrossRef](#)]
59. Yamamoto, N.; Matsuyama, S.; Hoshino, T.; Yamamoto, N. Nelfinavir inhibits replication of severe acute respiratory syndrome coronavirus 2 in vitro. *bioRxiv* **2020**. [[CrossRef](#)]
60. Mollica, V.; Rizzo, A.; Massari, F. The pivotal role of TMPRSS2 in coronavirus disease 2019 and prostate cancer. *Future Oncol.* **2020**, *16*, 2029–2033. [[CrossRef](#)]
61. Kuteykin-Teplyakov, K.; Luna-Tortós, C.; Ambroziak, K.; Löscher, W. Differences in the expression of endogenous efflux transporters in MDR1-transfected versus wildtype cell lines affect P-glycoprotein mediated drug transport. *Br. J. Pharmacol.* **2010**, *160*, 1453–1463. [[CrossRef](#)]
62. Tummino, T.A.; Rezelj, V.V.; Fischer, B.; Fischer, A.; O'Meara, M.J.; Monel, B.; Vallet, T.; Zhang, Z.; Alon, A.; O'Donnell, H.R.; et al. Drug-induced phospholipidosis confounds drug repurposing for SARS-CoV-2. *Science* **2021**, *373*, 541–547. [[CrossRef](#)]
63. Dittmar, M.; Lee, J.S.; Whig, K.; Segrist, E.; Li, M.; Kamalia, B.; Castellana, L.; Ayyanathan, K.; Cardenas-Diaz, F.L.; Morrissey, E.E.; et al. Drug repurposing screens reveal cell-type-specific entry pathways and FDA-approved drugs active against SARS-Cov-2. *Cell Rep.* **2021**, *35*, 108959. [[CrossRef](#)]

64. Lukassen, S.; Chua, R.L.; Trefzer, T.; Kahn, N.C.; Schneider, M.A.; Muley, T.; Winter, H.; Meister, M.; Veith, C.; Boots, A.W.; et al. SARS-CoV-2 receptor ACE2 and TMPRSS2 are primarily expressed in bronchial transient secretory cells. *EMBO J.* **2020**, *39*, e105114. [CrossRef] [PubMed]
65. Hoffmann, M.; Kleine-Weber, H.; Schroeder, S.; Krüger, N.; Herrler, T.; Erichsen, S.; Schiergens, T.S.; Herrler, G.; Wu, N.H.; Nitsche, A.; et al. SARS-CoV-2 Cell Entry Depends on ACE2 and TMPRSS2 and Is Blocked by a Clinically Proven Protease Inhibitor. *Cell* **2020**, *181*, 271–280.e8. [CrossRef] [PubMed]
66. Atea Pharmaceuticals Press Release. Atea Pharmaceuticals Provides Update and Topline Results for Phase 2 MOONSONG Trial Evaluating AT-527 in the Outpatient Setting. 19 October 2021. Available online: <https://ir.ateapharma.com/news-releases/news-release-details/atea-pharmaceuticals-provides-update-and-topline-results-phase-2> (accessed on 24 June 2022).
67. Neervannan, S. Preclinical formulations for discovery and toxicology: Physicochemical challenges. *Expert Opin. Drug Metab. Toxicol.* **2006**, *2*, 715–731. [CrossRef] [PubMed]
68. Møhlhave, M.; Agergaard, J.; Wejse, C. Clinical Management of COVID-19 Patients—An Update. *Semin. Nucl. Med.* **2022**, *52*, 4–10. [CrossRef] [PubMed]
69. Richardson, C.; Bhagani, S.; Pollara, G. Antiviral treatment for COVID-19: The evidence supporting remdesivir. *Clin. Med.* **2020**, *20*, e215–e217. [CrossRef]
70. Good, S.S.; Westover, J.; Jung, K.H.; Zhou, X.J.; Moussa, A.; La Colla, P.; Collu, G.; Canard, B.; Sommadossi, J.P. AT-527, a Double Prodrug of a Guanosine Nucleotide Analog, Is a Potent Inhibitor of SARS-CoV-2 In Vitro and a Promising Oral Antiviral for Treatment of COVID-19. *Antimicrob. Agents Chemother.* **2021**, *65*, e02479–20. [CrossRef]
71. Collins, F.S. COVID-19 lessons for research. *Science* **2021**, *371*, 1081. [CrossRef]
72. Mullard, A. RECOVERY 1 year on: A rare success in the COVID-19 clinical trial landscape. *Nat. Rev. Drug Discov.* **2021**, *20*, 336–337. [CrossRef]
73. Axfors, C.; Schmitt, A.M.; Janiaud, P.; Van't Hooft, J.; Abd-Elsalam, S.; Abdo, E.F.; Abella, B.S.; Akram, J.; Amaravadi, R.K.; Angus, D.C.; et al. Mortality outcomes with hydroxychloroquine and chloroquine in COVID-19 from an international collaborative meta-analysis of randomized trials. *Nat. Commun.* **2021**, *12*, 2349. [CrossRef]
74. Mobarak, S.; Salasi, M.; Hormati, A.; Khodadadi, J.; Ziaee, M.; Abedi, F.; Ebrahimzadeh, A.; Azarkar, Z.; Mansour-Ghanaei, F.; Joukar, F.; et al. Evaluation of the effect of sofosbuvir and daclatasvir in hospitalized COVID-19 patients: A randomized double-blind clinical trial (DISCOVER). *J. Antimicrob. Chemother.* **2022**, *77*, 758–766. [CrossRef]
75. Patel, T.K.; Patel, P.B.; Barvaliya, M.; Saurabh, M.K.; Bhalla, H.L.; Khosla, P.P. Efficacy and safety of lopinavir-ritonavir in COVID-19: A systematic review of randomized controlled trials. *J. Infect. Public Health* **2021**, *14*, 740–748. [CrossRef] [PubMed]
76. Acharya, B.N. Amodiaquine as COVID-19 Mpro Inhibitor: A Theoretical Study. *ChemRxiv* **2020**. [CrossRef]
77. World Health Organization. Tracking SARS-CoV-2 Variants. Available online: <https://www.who.int/activities/tracking-SARS-CoV-2-variants> (accessed on 23 June 2022).
78. World Health Organization. Facilitation Council Preparation. 19 March 2021. Available online: https://www.who.int/docs/default-source/coronaviruse/act-accelerator/act-a-tx-dx-fc-pre-briefing-deck_fin.pdf?sfvrsn=ce5b7dea_1&download=true (accessed on 5 May 2022).
79. World Health Organization. Therapeutics and COVID-19: Living Guideline. 22 April 2022. Available online: <https://www.who.int/publications/i/item/WHO-2019-nCoV-therapeutics-2022.3> (accessed on 15 June 2022).
80. Jochmans, D.; Leyssen, P.; Neyts, J. A novel method for high-throughput screening to quantify antiviral activity against viruses that induce limited CPE. *J. Virol. Methods* **2012**, *183*, 176–179. [CrossRef] [PubMed]
81. Touret, F.; Driouich, J.S.; Cochin, M.; Petit, P.R.; Gilles, M.; Barthélémy, K.; Moureau, G.; Mahon, F.X.; Malvy, D.; Solas, C.; et al. Preclinical evaluation of Imatinib does not support its use as an antiviral drug against SARS-CoV-2. *Antivir. Res.* **2021**, *193*, 105137. [CrossRef] [PubMed]
82. Pizzorno, A.; Padey, B.; Julien, T.; Trouillet-Assant, S.; Traversier, A.; Errazuriz-Cerda, E.; Fouret, J.; Dubois, J.; Gaymard, A.; Lescure, F.X.; et al. Characterization and Treatment of SARS-CoV-2 in Nasal and Bronchial Human Airway Epithelia. *Cell Rep. Med.* **2020**, *1*, 100059. [CrossRef] [PubMed]
83. Gruber, A.D.; Firsching, T.C.; Trimpert, J.; Dietert, K. Hamster models of COVID-19 pneumonia reviewed: How human can they be? *Vet. Pathol.* **2022**, *59*, 528–545. [CrossRef] [PubMed]
84. Sia, S.F.; Yan, L.M.; Chin, A.W.H.; Fung, K.; Choy, K.T.; Wong, A.Y.L.; Kaewpreedee, P.; Perera, R.; Poon, L.L.M.; Nicholls, J.M.; et al. Pathogenesis and transmission of SARS-CoV-2 in golden hamsters. *Nature* **2020**, *583*, 834–838. [CrossRef] [PubMed]
85. Francis, M.E.; Goncin, U.; Kroeker, A.; Swan, C.; Ralph, R.; Lu, Y.; Etzioni, A.L.; Falzarano, D.; Gerdtts, V.; Machtaler, S.; et al. SARS-CoV-2 infection in the Syrian hamster model causes inflammation as well as type I interferon dysregulation in both respiratory and non-respiratory tissues including the heart and kidney. *PLoS Pathog.* **2021**, *17*, e1009705. [CrossRef] [PubMed]
86. Sheahan, T.P.; Sims, A.C.; Zhou, S.; Graham, R.L.; Pruijssers, A.J.; Agostini, M.L.; Leist, S.R.; Schäfer, A.; Dinno, K.H., 3rd; Stevens, L.J.; et al. An orally bioavailable broad-spectrum antiviral inhibits SARS-CoV-2 in human airway epithelial cell cultures and multiple coronaviruses in mice. *Sci. Transl. Med.* **2020**, *12*, eabb5883. [CrossRef] [PubMed]
87. Cox, R.M.; Wolf, J.D.; Plemper, R.K. Therapeutically administered ribonucleoside analogue MK-4482/EIDD-2801 blocks SARS-CoV-2 transmission in ferrets. *Nat. Microbiol.* **2021**, *6*, 11–18. [CrossRef]

88. Sheahan, T.P.; Sims, A.C.; Graham, R.L.; Menachery, V.D.; Gralinski, L.E.; Case, J.B.; Leist, S.R.; Pyrc, K.; Feng, J.Y.; Trantcheva, I.; et al. Broad-spectrum antiviral GS-5734 inhibits both epidemic and zoonotic coronaviruses. *Sci. Transl. Med.* **2017**, *9*, eaal3653. [[CrossRef](#)]
89. Pruijssers, A.J.; George, A.S.; Schäfer, A.; Leist, S.R.; Gralinski, L.E.; Dinnon, K.H., 3rd; Yount, B.L.; Agostini, M.L.; Stevens, L.J.; Chappell, J.D.; et al. Remdesivir Inhibits SARS-CoV-2 in Human Lung Cells and Chimeric SARS-CoV Expressing the SARS-CoV-2 RNA Polymerase in Mice. *Cell Rep.* **2020**, *32*, 107940. [[CrossRef](#)] [[PubMed](#)]
90. Abdelnabi, R.; Boudewijns, R.; Foo, C.S.; Seldeslachts, L.; Sanchez-Felipe, L.; Zhang, X.; Delang, L.; Maes, P.; Kaptein, S.J.F.; Weynand, B.; et al. Comparing infectivity and virulence of emerging SARS-CoV-2 variants in Syrian hamsters. *EBioMedicine* **2021**, *68*, 103403. [[CrossRef](#)] [[PubMed](#)]
91. Cochin, M.; Luciani, L.; Touret, F.; Driouich, J.S.; Petit, P.R.; Moureau, G.; Baronti, C.; Laprie, C.; Thirion, L.; Maes, P.; et al. The SARS-CoV-2 Alpha variant exhibits comparable fitness to the D614G strain in a Syrian hamster model. *Commun. Biol.* **2022**, *5*, 225. [[CrossRef](#)] [[PubMed](#)]
92. Cochin, M.; Touret, F.; Driouich, J.S.; Moureau, G.; Petit, P.R.; Laprie, C.; Solas, C.; de Lamballerie, X.; Nougairède, A. Hydroxychloroquine and azithromycin used alone or combined are not effective against SARS-CoV-2 ex vivo and in a hamster model. *Antivir. Res.* **2022**, *197*, 105212. [[CrossRef](#)]
93. Driouich, J.-S.; Cochin, M.; Touret, F.; Petit, P.-R.; Gilles, M.; Moureau, G.; Barthélémy, K.; Laprie, C.; Wattanakul, T.; Chotsiri, P.; et al. Pre-clinical evaluation of antiviral activity of nitazoxanide against Sars-CoV-2. *EBioMedicine* **2022**, *82*, 104148. [[CrossRef](#)]
94. Savic, R.M.; Jonker, D.M.; Kerbusch, T.; Karlsson, M.O. Implementation of a transit compartment model for describing drug absorption in pharmacokinetic studies. *J. Pharmacokinet. Pharmacodyn.* **2007**, *34*, 711–726. [[CrossRef](#)] [[PubMed](#)]
95. Dosne, A.G.; Bergstrand, M.; Karlsson, M.O. An automated sampling importance resampling procedure for estimating parameter uncertainty. *J. Pharmacokinet. Pharmacodyn.* **2017**, *44*, 509–520. [[CrossRef](#)] [[PubMed](#)]
96. Ferreira Sales-Medina, D.; Rodrigues Pinto Ferreira, L.; Romera, L.M.D.; Ribeiro Gonçalves, K.; Guido, R.V.C.; Courtemanche, G.; Buckeridge, M.S.; Durigon, E.L.; Moraes, C.B.; Freitas-Junior, L.H. Discovery of clinically approved drugs capable of inhibiting SARS-CoV-2 in vitro infection using a phenotypic screening strategy and network-analysis to predict their potential to treat covid-19. *bioRxiv* **2020**. [[CrossRef](#)]
97. Jeon, S.; Ko, M.; Lee, J.; Choi, I.; Byun, S.Y.; Park, S.; Shum, D.; Kim, S. Identification of Antiviral Drug Candidates against SARS-CoV-2 from FDA-Approved Drugs. *Antimicrob. Agents Chemother.* **2020**, *64*. [[CrossRef](#)] [[PubMed](#)]
98. Sacramento, C.Q.; Fintelman-Rodrigues, N.; Temerozo, J.R.; Da Silva, A.P.D.; Dias, S.; da Silva, C.D.S.; Ferreira, A.C.; Mattos, M.; Pao, C.R.R.; de Freitas, C.S.; et al. In vitro antiviral activity of the anti-HCV drugs daclatasvir and sofosbuvir against SARS-CoV-2, the aetiological agent of COVID-19. *J. Antimicrob. Chemother.* **2021**, *76*, 1874–1885. [[CrossRef](#)] [[PubMed](#)]
99. Ko, M.; Jeon, S.; Ryu, W.S.; Kim, S. Comparative analysis of antiviral efficacy of FDA-approved drugs against SARS-CoV-2 in human lung cells. *J. Med. Virol.* **2021**, *93*, 1403–1408. [[CrossRef](#)] [[PubMed](#)]
100. Weston, S.; Coleman, C.M.; Haupt, R.; Logue, J.; Matthews, K.; Li, Y.; Reyes, H.M.; Weiss, S.R.; Frieman, M.B. Broad Anticoronavirus Activity of Food and Drug Administration-Approved Drugs against SARS-CoV-2 In Vitro and SARS-CoV In Vivo. *J. Virol.* **2020**, *94*, e01218-20. [[CrossRef](#)] [[PubMed](#)]
101. Choy, K.T.; Wong, A.Y.; Kaewpreedee, P.; Sia, S.F.; Chen, D.; Hui, K.P.Y.; Chu, D.K.W.; Chan, M.C.W.; Cheung, P.P.; Huang, X.; et al. Remdesivir, lopinavir, emetine, and homoharringtonine inhibit SARS-CoV-2 replication in vitro. *Antivir. Res.* **2020**, *178*, 104786. [[CrossRef](#)] [[PubMed](#)]
102. Liu, S.; Lien, C.Z.; Selvaraj, P.; Wang, T.T. Evaluation of 19 antiviral drugs against SARS-CoV-2 Infection. *BioRxiv* **2020**. [[CrossRef](#)]
103. Shannon, A.; Selisko, B.; Le, N.T.; Huchting, J.; Touret, F.; Piorkowski, G.; Fattorini, V.; Ferron, F.; Decroly, E.; Meier, C.; et al. Rapid incorporation of Favipiravir by the fast and permissive viral RNA polymerase complex results in SARS-CoV-2 lethal mutagenesis. *Nat. Commun.* **2020**, *11*, 4682. [[CrossRef](#)] [[PubMed](#)]
104. Wang, M.; Cao, R.; Zhang, L.; Yang, X.; Liu, J.; Xu, M.; Shi, Z.; Hu, Z.; Zhong, W.; Xiao, G. Remdesivir and chloroquine effectively inhibit the recently emerged novel coronavirus (2019-nCoV) in vitro. *Cell Res.* **2020**, *30*, 269–271. [[CrossRef](#)] [[PubMed](#)]
105. Zandi, K.; Amblard, F.; Musall, K.; Downs-Bowen, J.; Kleinbard, R.; Oo, A.; Cao, D.; Liang, B.; Russell, O.O.; McBrayer, T.; et al. Repurposing Nucleoside Analogs for Human Coronaviruses. *Antimicrob. Agents Chemother.* **2020**, *65*, e01652-20. [[CrossRef](#)]
106. Caly, L.; Druce, J.D.; Catton, M.G.; Jans, D.A.; Wagstaff, K.M. The FDA-approved drug ivermectin inhibits the replication of SARS-CoV-2 in vitro. *Antivir. Res.* **2020**, *178*, 104787. [[CrossRef](#)]
107. Jeffreys, L.N.; Pennington, S.H.; Duggan, J.; Caygill, C.H.; Lopeman, R.C.; Breen, A.F.; Jinks, J.B.; Ardrey, A.; Donnellan, S.; Patterson, E.I.; et al. Remdesivir-ivermectin combination displays synergistic interaction with improved in vitro activity against SARS-CoV-2. *Int. J. Antimicrob. Agents* **2022**, *59*, 106542. [[CrossRef](#)] [[PubMed](#)]
108. Yamamoto, N.; Yang, R.; Yoshinaka, Y.; Amari, S.; Nakano, T.; Cinatl, J.; Rabenau, H.; Doerr, H.W.; Hunsmann, G.; Otaka, A.; et al. HIV protease inhibitor nelfinavir inhibits replication of SARS-associated coronavirus. *Biochem. Biophys. Res. Commun.* **2004**, *318*, 719–725. [[CrossRef](#)] [[PubMed](#)]
109. Xu, Z.; Yao, H.; Shen, J.; Wu, N.; Xu, Y.; Lu, X.; Zhu, W.; Li, L.-J. Nelfinavir Is Active Against SARS-CoV-2 in Vero E6 Cells. *ChemRxiv* **2020**.
110. Rogosnitzky, M.; Danks, R. Therapeutic potential of the biscoclaurine alkaloid, cepharanthine, for a range of clinical conditions. *Pharmacol. Rep.* **2011**, *63*, 337–347. [[CrossRef](#)]

111. Zimniak, M.; Kirschner, L.; Hilpert, H.; Geiger, N.; Danov, O.; Oberwinkler, H.; Steinke, M.; Sewald, K.; Seibel, J.; Bodem, J. The serotonin reuptake inhibitor Fluoxetine inhibits SARS-CoV-2 in human lung tissue. *Sci. Rep.* **2021**, *11*, 5890. [CrossRef]
112. Schloer, S.; Brunotte, L.; Goretzko, J.; Mecate-Zambrano, A.; Korthals, N.; Gerke, V.; Ludwig, S.; Rescher, U. Targeting the endolysosomal host-SARS-CoV-2 interface by clinically licensed functional inhibitors of acid sphingomyelinase (FIASMA) including the antidepressant fluoxetine. *Emerg. Microbes Infect.* **2020**, *9*, 2245–2255. [CrossRef]
113. Fred, S.M.; Kuivanen, S.; Ugurlu, H.; Casarotto, P.C.; Levanov, L.; Saksela, K.; Vapalahti, O.; Castren, E. Antidepressant and Antipsychotic Drugs Reduce Viral Infection by SARS-CoV-2 and Fluoxetine Shows Antiviral Activity Against the Novel Variants in vitro. *Front. Pharmacol.* **2021**, *12*, 755600. [CrossRef] [PubMed]
114. Olaleye, O.A.; Kaur, M.; Onyenaka, C.C. Ambroxol Hydrochloride Inhibits the Interaction between Severe Acute Respiratory Syndrome Coronavirus 2 Spike Protein's Receptor Binding Domain and Recombinant Human ACE2. *BioRxiv* **2020**. [CrossRef]
115. Mahoney, M.; Damalanka, V.C.; Tartell, M.A.; Chung, D.H.; Lourenco, A.L.; Pwee, D.; Mayer Bridwell, A.E.; Hoffmann, M.; Voss, J.; Karmakar, P.; et al. A novel class of TMPRSS2 inhibitors potentially block SARS-CoV-2 and MERS-CoV viral entry and protect human epithelial lung cells. *Proc. Natl. Acad. Sci. USA* **2021**, *118*, e2108728118. [CrossRef] [PubMed]
116. Schultz, D.C.; Johnson, R.M.; Ayyanathan, K.; Miller, J.; Whig, K.; Kamalia, B.; Dittmar, M.; Weston, S.; Hammond, H.L.; Dillen, C.; et al. Pyrimidine inhibitors synergize with nucleoside analogues to block SARS-CoV-2. *Nature* **2022**, *604*, 134–140. [CrossRef]
117. Owen, D.R.; Allerton, C.M.N.; Anderson, A.S.; Aschenbrenner, L.; Avery, M.; Berritt, S.; Boras, B.; Cardin, R.D.; Carlo, A.; Coffman, K.J.; et al. An oral SARS-CoV-2 M(pro) inhibitor clinical candidate for the treatment of COVID-19. *Science* **2021**, *374*, 1586–1593. [CrossRef]
118. Xiong, R.; Zhang, L.; Li, S.; Sun, Y.; Ding, M.; Wang, Y.; Zhao, Y.; Wu, Y.; Shang, W.; Jiang, X.; et al. Novel and potent inhibitors targeting DHODH are broad-spectrum antivirals against RNA viruses including newly-emerged coronavirus SARS-CoV-2. *Protein Cell* **2020**, *11*, 723–739. [CrossRef] [PubMed]
119. Swaim, C.D.; Dwivedi, V.; Perng, Y.C.; Zhao, X.; Canadeo, L.A.; Harastani, H.H.; Darling, T.L.; Boon, A.C.M.; Lenschow, D.J.; Kulkarni, V.; et al. 6-Thioguanine blocks SARS-CoV-2 replication by inhibition of PLpro. *iScience* **2021**, *24*, 103213. [CrossRef] [PubMed]
120. McCoy, J.; Goren, A.; Cadejani, F.A.; Vaño-Galván, S.; Kovacevic, M.; Situm, M.; Shapiro, J.; Sinclair, R.; Tosti, A.; Stanimirovic, A.; et al. Proxalutamide Reduces the Rate of Hospitalization for COVID-19 Male Outpatients: A Randomized Double-Blinded Placebo-Controlled Trial. *Front. Med.* **2021**, *8*, 668698. [CrossRef]
121. Murray, J.; Hogan, R.J.; Martin, D.E.; Blahunka, K.; Sancilio, F.D.; Balyan, R.; Lovern, M.; Still, R.; Tripp, R.A. Probenecid inhibits SARS-CoV-2 replication in vivo and in vitro. *Sci. Rep.* **2021**, *11*, 18085. [CrossRef] [PubMed]
122. Box, H.; Pennington, S.H.; Kijak, E.; Tatham, L.; Caygill, C.H.; Lopeman, R.C.; Jeffrey, L.N.; Herriott, J.; Sharp, J.; Neary, M.; et al. Lack of antiviral activity of probenecid in Vero E6 cells and Syrian golden hamsters: A need for better understanding of inter-lab differences in preclinical assays. *bioRxiv* **2022**. [CrossRef]
123. Muturi, E.; Hong, W.; Li, J.; Yang, W.; He, J.; Wei, H.; Yang, H. Effects of simeprevir on the replication of SARS-CoV-2 in vitro and in transgenic hACE2 mice. *Int. J. Antimicrob. Agents* **2022**, *59*, 106499. [CrossRef]
124. Abdelnabi, R.; Foo, C.S.; Kaptein, S.J.F.; Zhang, X.; Do, T.N.D.; Langendries, L.; Vangeel, L.; Breuer, J.; Pang, J.; Williams, R.; et al. The combined treatment of Molnupiravir and Favipiravir results in a potentiation of antiviral efficacy in a SARS-CoV-2 hamster infection model. *EBioMedicine* **2021**, *72*, 103595. [CrossRef]
125. Jan, J.T.; Cheng, T.R.; Juang, Y.P.; Ma, H.H.; Wu, Y.T.; Yang, W.B.; Cheng, C.W.; Chen, X.; Chou, T.H.; Shie, J.J.; et al. Identification of existing pharmaceuticals and herbal medicines as inhibitors of SARS-CoV-2 infection. *Proc. Natl. Acad. Sci. USA* **2021**, *118*, e2021579118. [CrossRef]
126. Arevalo, A.P.; Pagotto, R.; Porfido, J.L.; Daghero, H.; Segovia, M.; Yamasaki, K.; Varela, B.; Hill, M.; Verdes, J.M.; Duhalde Vega, M.; et al. Ivermectin reduces in vivo coronavirus infection in a mouse experimental model. *Sci. Rep.* **2021**, *11*, 7132. [CrossRef]
127. Pussard, E.; Verdier, F. Antimalarial 4-aminoquinolines: Mode of action and pharmacokinetics. *Fundam. Clin. Pharmacol.* **1994**, *8*, 1–17. [CrossRef]
128. Atazanavir PK Fact Sheet. Available online: https://liverpool-hiv-hep.s3.amazonaws.com/fact_sheets/pdfs/000/000/087/original/HIV_FactSheet_ATV_2016_Mar.pdf (accessed on 1 July 2022).
129. Gandhi, Y.; Eley, T.; Fura, A.; Li, W.; Bertz, R.J.; Garimella, T. Daclatasvir: A Review of Preclinical and Clinical Pharmacokinetics. *Clin. Pharmacokinet.* **2018**, *57*, 911–928. [CrossRef] [PubMed]
130. Hayden, F.G.; Shindo, N. Influenza virus polymerase inhibitors in clinical development. *Curr. Opin. Infect. Dis.* **2019**, *32*, 176–186. [CrossRef]
131. González Canga, A.; Sahagún Prieto, A.M.; Diez Liébana, M.J.; Fernández Martínez, N.; Sierra Vega, M.; García Vieitez, J.J. The pharmacokinetics and interactions of ivermectin in humans—A mini-review. *AAPS J.* **2008**, *10*, 42–46. [CrossRef] [PubMed]
132. Romark Pharmaceuticals, Alinia[®], Product Monograph. 2005. Available online: https://www.accessdata.fda.gov/drugsatfda_docs/label/2005/021818lbl.pdf (accessed on 1 July 2022).
133. Cada, D.J.; Cong, J.; Baker, D.E. Sofosbuvir. *Hosp. Pharm.* **2014**, *49*, 466–478. [CrossRef]
134. Lee, H.J.; Joung, S.K.; Kim, Y.G.; Yoo, J.Y.; Han, S.B. Bioequivalence assessment of ambroxol tablet after a single oral dose administration to healthy male volunteers. *Pharmacol. Res.* **2004**, *49*, 93–98. [CrossRef] [PubMed]

135. Tarning, J.; Chotsiri, P.; Jullien, V.; Rijken, M.J.; Bergstrand, M.; Cammas, M.; McGready, R.; Singhasivanon, P.; Day, N.P.; White, N.J.; et al. Population pharmacokinetic and pharmacodynamic modeling of amodiaquine and desethylamodiaquine in women with *Plasmodium vivax* malaria during and after pregnancy. *Antimicrob. Agents Chemother.* **2012**, *56*, 5764–5773. [[CrossRef](#)] [[PubMed](#)]
136. Punyawudho, B.; Thammajarak, N.; Ruxrungtham, K.; Avihingsanon, A. Population pharmacokinetics and dose optimisation of ritonavir-boosted atazanavir in Thai HIV-infected patients. *Int. J. Antimicrob. Agents* **2017**, *49*, 327–332. [[CrossRef](#)]
137. Hao, G.; Liang, H.; Li, Y.; Li, H.; Gao, H.; Liu, G.; Liu, Z. Simple, sensitive and rapid HPLC-MS/MS method for the determination of cepharanthine in human plasma. *J. Chromatogr. B* **2010**, *878*, 2923–2927. [[CrossRef](#)]
138. Yasuda, K.; Moro, M.; Akasu, M.; Ohnishi, A. Pharmacokinetic disposition of cepharanthin following single and multiple intravenous doses in healthy subjects. *Jpn. J. Clin. Pharmacol. Ther.* **1989**, *20*, 741–749. [[CrossRef](#)]
139. Yasuda, K.; Moro, M.; Ohnishi, A.; Akasu, M.; Shishido, A.; Tsunoo, M. Pharmacokinetic study of cepharanthin following single oral doses in healthy subjects. *Jpn. J. Clin. Pharmacol. Ther.* **1989**, *20*, 735–740. [[CrossRef](#)]
140. Faraj, A.; Svensson, R.J.; Diacon, A.H.; Simonsson, U.S.H. Drug Effect of Clofazimine on Persisters Explains an Unexpected Increase in Bacterial Load in Patients. *Antimicrob. Agents Chemother.* **2020**, *64*, e01905-19. [[CrossRef](#)] [[PubMed](#)]
141. Chan, P.; Li, H.; Zhu, L.; Bifano, M.; Eley, T.; Osawa, M.; Ueno, T.; Hughes, E.; Bertz, R.; Garimella, T.; et al. Population Pharmacokinetic Analysis of Daclatasvir in Subjects with Chronic Hepatitis C Virus Infection. *Clin. Pharmacokinet.* **2017**, *56*, 1173–1183. [[CrossRef](#)]
142. Wang, Y.; Zhong, W.; Salam, A.; Tarning, J.; Zhan, Q.; Huang, J.A.; Weng, H.; Bai, C.; Ren, Y.; Yamada, K.; et al. Phase 2a, open-label, dose-escalating, multi-center pharmacokinetic study of favipiravir (T-705) in combination with oseltamivir in patients with severe influenza. *EBioMedicine* **2020**, *62*, 103125. [[CrossRef](#)] [[PubMed](#)]
143. Sagahón-Azúa, J.; Medellín-Garibay, S.E.; Chávez-Castillo, C.E.; González-Salinas, C.G.; Milán-Segovia, R.D.C.; Romano-Moreno, S. Factors associated with fluoxetine and norfluoxetine plasma concentrations and clinical response in Mexican patients with mental disorders. *Pharmacol. Res. Perspect.* **2021**, *9*, e00864. [[CrossRef](#)] [[PubMed](#)]
144. Orlando, R.; De Martin, S.; Andrighetto, L.; Floreani, M.; Palatini, P. Fluvoxamine pharmacokinetics in healthy elderly subjects and elderly patients with chronic heart failure. *Br. J. Clin. Pharmacol.* **2010**, *69*, 279–286. [[CrossRef](#)]
145. Kobylinski, K.C.; Ubalee, R.; Ponlawat, A.; Nitatsukprasert, C.; Phasomkulsolsil, S.; Wattanakul, T.; Tarning, J.; Na-Bangchang, K.; McCardle, P.W.; Davidson, S.A.; et al. Ivermectin susceptibility and sporontocidal effect in Greater Mekong Subregion *Anopheles*. *Malar. J.* **2017**, *16*, 280. [[CrossRef](#)]
146. Painter, W.P.; Holman, W.; Bush, J.A.; Almazedi, F.; Malik, H.; Eraut, N.; Morin, M.J.; Szewczyk, L.J.; Painter, G.R. Human Safety, Tolerability, and Pharmacokinetics of Molnupiravir, a Novel Broad-Spectrum Oral Antiviral Agent with Activity Against SARS-CoV-2. *Antimicrob. Agents Chemother.* **2021**, *65*, e02428-20. [[CrossRef](#)]
147. Hirt, D.; Treluyer, J.M.; Jullien, V.; Firtion, G.; Chappuy, H.; Rey, E.; Pons, G.; Mandelbrot, L.; Urien, S. Pregnancy-related effects on nelfinavir-M8 pharmacokinetics: A population study with 133 women. *Antimicrob. Agents Chemother.* **2006**, *50*, 2079–2086. [[CrossRef](#)]
148. Rajoli, R.K.R.; Pertinez, H.; Arshad, U.; Box, H.; Tatham, L.; Curley, P.; Neary, M.; Sharp, J.; Liptrott, N.J.; Valentijn, A.; et al. Dose prediction for repurposing nitazoxanide in SARS-CoV-2 treatment or chemoprophylaxis. *Br. J. Clin. Pharmacol.* **2021**, *87*, 2078–2088. [[CrossRef](#)]
149. Balderas-Acata, J.; Bueno, E.; Pérez-Becerril, F.; Espinosa-Martínez, C.; Burkefraga, V.; González-de la Parra, M. Bioavailability of Two Oral-Suspension Formulations of a Single Dose of Nitazoxanide 500 mg: An Open-Label, Randomized-Sequence, Two-Period Crossover, Comparison in Healthy Fasted Mexican Adult Volunteers. *J. Bioequiv. Bioavailab.* **2011**, *3*. [[CrossRef](#)]
150. Jin, F.; Kirby, B.; Gao, Y.; Kearney, B.; Mathias, A. Population Pharmacokinetic Modeling of Sofosbuvir, an NS5B Polymerase Inhibitor, and Its Metabolites in Patients with Hepatitis C Virus Infection, Poster presentation at PAGE-Meeting. 2015. Hersonissos, Crete, Greece. Available online: https://www.page-meeting.org/pdf_assets/3129-PAGE%20poster.pdf (accessed on 1 July 2022).
151. Rogosnitzky, M.; Okediji, P.; Koman, I. Cepharanthine: A review of the antiviral potential of a Japanese-approved alopecia drug in COVID-19. *Pharmacol. Rep.* **2020**, *72*, 1509–1516. [[CrossRef](#)] [[PubMed](#)]